

Copyright
by
Harshad Suresh Desai
2012

**The Thesis Committee for Harshad Suresh Desai
Certifies that this is the approved version of the following thesis:**

Point-of-load Converters for a Residential DC Distribution System

**APPROVED BY
SUPERVISING COMMITTEE:**

Supervisor:

Alexis Kwasinski

W. Mack Grady

Point-of-load Converters for a Residential DC Distribution System

by

Harshad Suresh Desai, B. Tech.

Thesis

Presented to the Faculty of the Graduate School of

The University of Texas at Austin

in Partial Fulfillment

of the Requirements

for the Degree of

Master of Science in Engineering

The University of Texas at Austin

May 2012

Dedicated to Aai and Pappa

Acknowledgements

I am grateful to Professor Alexis Kwasinski for his guidance and support throughout the duration of my Master's course. His research has given me great insights in understanding the theoretical and practical aspects of power electronics. His courses 'Advance Power Electronics' and 'Distributed Generation' have equipped me with skills and aptitude for research in power electronics and were instrumental in identifying the topic for this work. I would also like to thank him for providing me the resources needed in completion of this work.

I am thankful to Professor W. Mack Grady for his invaluable time in review of this thesis. I am also thankful to all my teachers who have inspired me over the years through their teaching and research.

I would like to thank my colleagues from Power Electronics Research Group: Sheng-Yang Yu, Ruichen Zhao, Harsha Kumar, Sungwoo Bae, Juyoung Jung, Vaidyanathan Krishnamurthy, Ted Song, Amir Toliyat and Myungchin Kim for their help during various stages of this work. I would like thank my friends Raghu, Neeraj, Libin, Varun and Ankit for their help and support.

Finally, I would like to express my gratitude to my parents, Lata and Suresh Desai for their constant encouragement and endless support. I am thankful to my younger brother, Chinmay, for all the interesting discussions and keeping me motivated.

Abstract

Point-of-load Converters for a Residential DC Distribution System

Harshad Suresh Desai, MSE

The University of Texas at Austin, 2012

Supervisor: Alexis Kwasinski

This thesis studies residential dc distribution system with primary focus on point-of-load (POL) converters. The growing number of inherently dc loads, increasing penetration of distributed energy resources (DERs) and advancements in power electronic converters are some of the reasons to reconsider the existing residential ac distribution system. A dc distribution system can achieve higher efficiency by eliminating the ac-dc rectifiers and power factor correction stages currently used in most domestic electronic appliances. In this thesis, 380V is identified as a suitable voltage level for the main dc bus. Safety issues are discussed and common domestic loads are characterized. Two common converter topologies – buck and flyback converters are suggested as POL converters for heating and LED lighting loads respectively. State-feedback control is designed and implemented for buck converter and current mode control of flyback converter is implemented. A 500W POL buck converter using state-feedback with integral control is designed and tested for heating load applications. Finally a small dc distribution system is simulated using the converter models. The response of the system is stable under load and line changes.

Table of Contents

List of Tables	ix
List of Figures	x
Chapter 1: Introduction	1
1.1 Motivation	1
1.2 DC distribution system	3
1.3 Thesis organization	6
Chapter 2: Residential DC Distribution System	7
2.1 Distribution System Configuration	7
2.1.1 Hybrid AC-DC system	8
2.1.2 DC-only system	9
2.2 Voltage Specifications and Safety Considerations	10
2.2.1 Voltage specification	10
2.2.2 Fault detection and safety issues	12
2.3 Characterization Of Domestic Electric Loads	13
2.3.1 Resistive or heating loads	13
2.3.2 Inductive or motor loads	14
2.3.3 Constant power or electronic loads	15
Chapter 3: Point-of-load Converters	18
3.1 Buck Converter	19
3.1.1 Linearized small-signal model of buck converter	20
3.1.2 State feedback control of buck converter	25
3.2 Flyback Converter	31
3.2.1 LED drivers	31
3.2.2 Flyback as POL converter for LED lighting loads	32

Chapter 4: Experimental Results of POL Buck Converter	39
Chapter 5: System Simulation Results.....	44
Chapter 6: Conclusions	49
References.....	51
Vita	55

List of Tables

Table 1:	A few common residential loads.....	14
Table 2:	Parameters used in simulation of buck converter.	24
Table 3:	Parameters used in simulation of flyback converter.	35
Table 4:	Efficiencies of individual POL converters at full load.	48

List of Figures

Figure 1:	Simplified residential AC distribution system.....	2
Figure 2:	Simplified residential DC distribution system.....	4
Figure 3:	Power distribution architecture (a) Centralized (b) Distributed – parallel configuration (c) Distributed – cascaded configuration.....	8
Figure 4:	Hybrid AC-DC distribution system.	9
Figure 5:	DC distribution system.	9
Figure 6:	Simple model for LED lighting loads, from [32].	16
Figure 7:	Buck converter.	19
Figure 8:	Circuit topology during (a) t_{on} i.e. $q(t) = 1$ and (b) during t_{off} i.e. $q(t) = 0$	20
Figure 9:	Circuit topology including non-idealities during (a) t_{on} i.e. $q(t) = 1$ and (b) during t_{off} i.e. $q(t) = 0$	22
Figure 10:	Open loop response of state-space average model.	24
Figure 11:	State-feedback control of buck converter.	26
Figure 12:	Circuit simulation of closed loop buck converter (a) output voltage with steady-state error (b) output voltage with a 5% step change in input voltage.....	27
Figure 13:	State-feedback with integral control of buck converter.	29
Figure 14:	Circuit simulation of closed loop buck converter with integral control (a) output voltage without steady-state error (b) output voltage with a 10% step change in input voltage.....	30
Figure 15:	Flyback converter.....	32

Figure 16:	Flyback converter (a) with transformer equivalent circuit (b) when $q(t)=1$ (c) when $q(t)=0$.	33
Figure 17:	Open loop response of flyback converter.	36
Figure 18:	Average current mode control of flyback converter.	37
Figure 19:	Closed loop flyback (a) output voltage (b) output current.	38
Figure 20:	Ripple in output voltage and inductor current when load current is (a) 5A (b) 2.5A.	40
Figure 21:	Response of converter due to step change in output current (a) from 2.5A to 5A (b) from 5A to 2.5A.	41
Figure 22:	Response of converter to changes in line voltage (a) E reduced to 342V (b) E increased to 400V.	42
Figure 23:	Converter efficiency over load range and at different bus voltage levels.	43
Figure 24:	DC distribution system with POL converters.	45
Figure 25:	Output voltage of the POL converters.	46
Figure 26:	Voltage response after 10% step change in bus voltage.	47
Figure 27:	Output of POL3 converter after load increase of 5A at 1A/ μ s.	47

Chapter 1: Introduction

DC distribution is quite common in isolated power systems like ships, electric vehicles, telecommunication power systems [1], and in small scale power systems like motherboard power distribution [2]. In recent years there has been an increasing interest in using similar distribution configuration at residential and commercial premises [2]-[8]. This chapter discusses the motivation for use of dc distribution in residential locations.

1.1 MOTIVATION

Figure 1 shows a modern day residential ac distribution system. The number of electronic loads that require direct current at the end stage namely computers, printers, portable consumer electronic devices has increased over the years [5], [8]. These loads are connected to the ac bus through a rectifier resulting in high harmonic content at the input. A power factor correction (PFC) stage is commonly used to reduce this harmonic content. The need for two stages increases the cost and reduces the efficiency. AC motors in washing machines, dish washers etc. which were traditionally supplied by alternating voltage are increasingly using variable speed drives (VSD) to improve the efficiency and to better control the speed of motors [2]. These VSDs use an intermediate dc stage for controlling the speed of motors as shown in Figure 1. Furthermore the improvements in LED based solid-state lighting technology will increase the use of ‘inherently dc’ loads [8]. This trend suggests most of the future domestic loads will be using dc at the last stage (computers, LED lighting) as well as an input stage to the inverter (VSD). Using an ac distribution system in such a case necessitates the use of a rectifier followed by power factor correction circuit. Increasing number of intermediary stages before electric energy can be used reduces the efficiency of existing ac distribution system.

Various technical, environmental and economic reasons have increased the penetration of small generation sources like rooftop solar (PV), fuel cells, micro-turbines, wind turbines and energy storage in form of plug-in hybrid vehicles, ultra-capacitors at the distribution stage [2]. Together these can be termed as distributed energy resources (DERs). Although the use of DERs in a home is not yet common, it is predicted to grow rapidly in near future [2], [8], so are included in Figure 1. Most of these DERs are dc sources while others like micro-turbines, wind turbines generally operate as high-frequency ac sources and require power electronic converters to interface with the grid. Interfacing DERs in an ac distribution system would require the use of dc-ac inverters and filters, as shown in Figure 1. These inverters and filters increase the number of stages before electric energy can be used thus reducing the overall system efficiency.

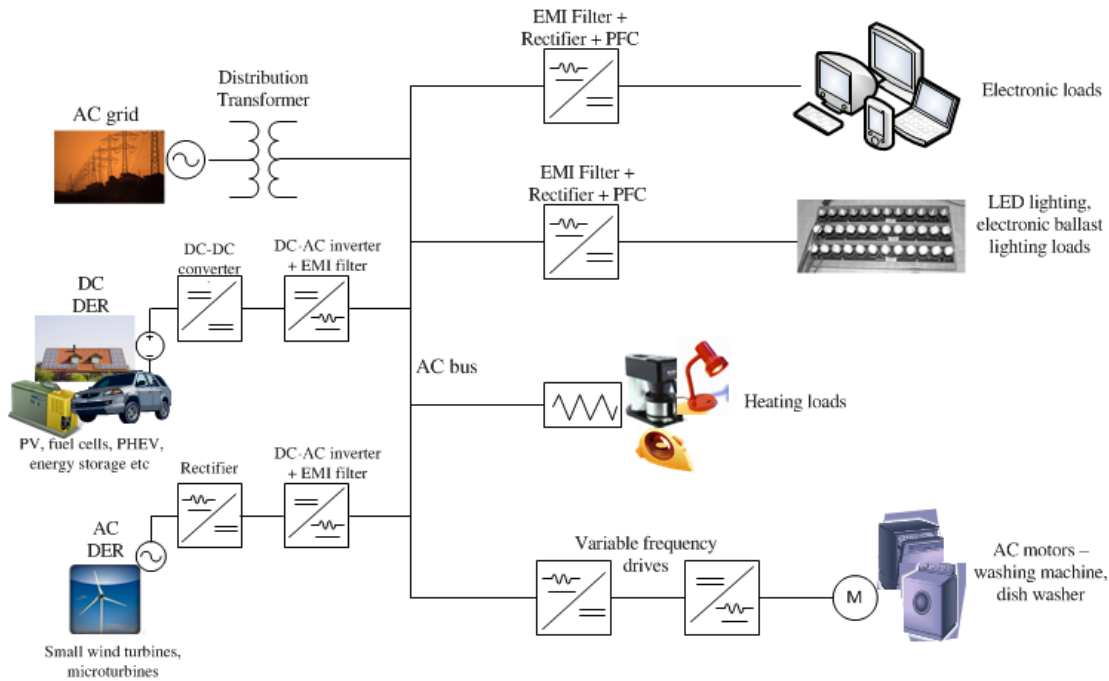


Figure 1: Simplified residential AC distribution system.

The interest in using power electronic converters to control the dynamics of power systems has grown over the years [2], [11], [25]. As proposed in [2], future electronic power distribution system would decouple the dynamics of generation, distribution and delivery of electric power achieved by using separate source converters, load converters and power distribution converters. These controllable converters are usually built-in with current limiting and current monitoring features. The ability to limit current can reduce the costs of electromechanical protection devices. Also current monitoring is an attractive feature from the perspective of home automation and home energy management systems provided appropriate communication protocols between converters are developed. Although these power converters can be incorporated in an ac system, the features of complete decoupling and reducing protection devices cannot be fully achieved in an ac system [2].

The ubiquity of inherently dc loads, increasing number of dc or power converter interfaced DERs and a growing interest in using power converters at generation, distribution and delivery stages motivates the use of dc distribution in residential and commercial premises.

1.2 DC DISTRIBUTION SYSTEM

DC distribution can be traced back to the early days of electric power generation and distribution. One of the earliest power systems, the Pearl Street power station, used 110V dc for generation, transmission and distribution [9]. With the invention of the induction motor and transformers, ac distribution prevailed for residential power systems. DC was restricted to isolated and geographically-small load centers like telecom power systems and railway applications. As the field of power electronics evolved over time, the issue of efficiently converting dc voltages was no longer a compromise. Along with the

advances in power electronics, more and more domestic electric loads started using dc power. This has rekindled the interest in residential dc distribution.

Figure 2 shows a residential dc distribution system [3]. In the shown configuration, it is assumed the grid still provides ac power. The rectification stage is now shifted at the distribution transformer stage thereby eliminating many small rectifiers and PFC circuits. The central high power front-end AC/DC rectifier operating at higher load is more efficient than several rectifiers operating at partial loading [5]. The electronic loads can be interfaced to the dc bus using a dc-dc converter. Heating loads can be connected directly to the dc bus as long as the dc voltage is equal to the RMS voltage in the ac system. The first rectification stage for ac motors is eliminated as well.

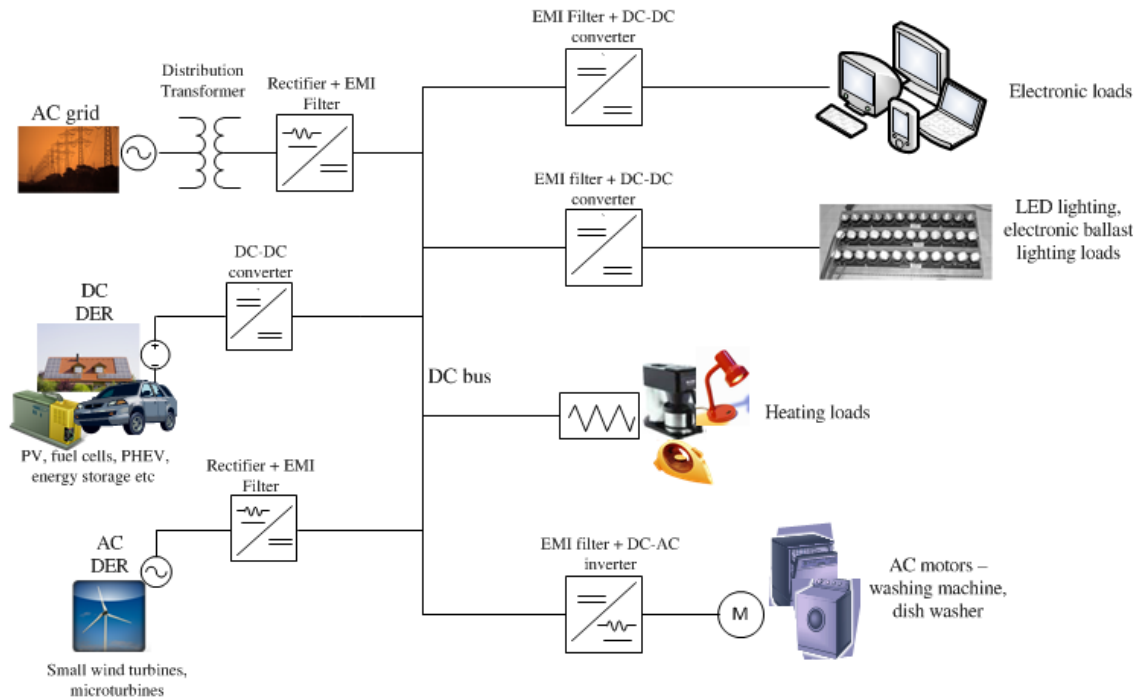


Figure 2: Simplified residential DC distribution system.

DC buses allow easier paralleling of different sources than ac buses [7]. AC sources require frequency and phase balance along with voltage balance making it difficult to parallel multiple DERs in an ac system. Using source converters for DERs the output can be made dc thus making it easier to parallel multiple DERs as shown in Figure 2. The converters for energy storage devices like PHEVs could be designed to have bi-directional power flow.

Various load converters are connected to the central dc bus. These load converters called point-of-load (POL) converters are able to precisely regulate the voltage at loads. This concept is similar to the one found in many distributed power system architectures like a computer motherboard power distribution [10]. Multiple POL converters improve the overall system efficiency and reduce cost and weight [2]. The dc bus can be allowed to have a wider voltage variation simplifying the design of central rectifier (or a dc-dc converter if grid supplies dc power). The wider bus voltage variation is also beneficial in incorporating energy storage elements like batteries. Using POL converters the loads can be dynamically decoupled and would allow load current monitoring enabling built-in protection features.

To realize the full advantages of a dc system the crucial aspects can be identified as:

- Lack of standards and safety concerns
- Studying the system architecture and system stability issues
- Designing power electronic converters based on the characteristics of loads and local generation sources

In dc distribution system, point-of-load converters are an important component as identified in [2], [3] and [10]. Delivering power efficiently at light loads is particularly important in a residential setting as most of the loads are inactive or in standby mode.

The POL converters must be designed based on the nature of loads keeping in mind the power requirement and dynamic response. This thesis proposes POL converters that can be used in a residential dc distribution system.

1.3 THESIS ORGANIZATION

The motivation for use of dc distribution at residential level was presented in previous sections. A system perspective of dc distribution is discussed in next chapter and later the individual point-of-load converters are studied. Chapter 2 surveys the different distribution architectures, voltage levels, standards and safety considerations for dc distribution. The various household loads are studied and characterized in this chapter.

Chapter 3 proposes a few simple well known topologies of dc-dc converters that can be used as point-of-load converters in a dc distribution system. Control for these converters is designed and simulation results are presented. Chapter 4 presents the experimental results of one such converter with the designed control system.

A system level simulation study of the proposed distribution system is presented in chapter 5. Various transient scenarios are studied and steady state efficiency results are provided.

Finally, chapter 6 presents the conclusions of this thesis and possible future work is outlined. This is followed by the list of references.

Chapter 2: Residential DC Distribution System

2.1 DISTRIBUTION SYSTEM CONFIGURATION

Power can be delivered to loads using either centralized or distributed architecture [7]. In a centralized architecture all power processing is done in a single stage. The line voltage is converted to different load voltages as shown in Figure 3(a). This simplifies electromagnetic interference and thermal management issues. However, centralized architecture may lead to single point of failure and is not favorable for load expansion. In a distributed architecture power is processed over multiple converters. Such architecture can have parallel or cascaded structure as shown in Figures 3 (b) and 3 (c) respectively. A parallel configuration uses load sharing to improve reliability. Multiple converters are paralleled to deliver power to the load. When loads increase, more power converters can be paralleled to meet the increased demand. In a cascaded architecture an intermediate voltage bus is used and multiple converters located close to load are used to provide point-of-load regulation generally resulting in two or more stages. The intermediate bus can be allowed to have wider voltage variation. Cascaded configuration can lead to better point-of-load regulation, improved dynamic response and improved system efficiency [10]. The first stage converters are called line conditioning converters (LCC) while downstream converters are referred to as point-of-load (POL) converters [7].

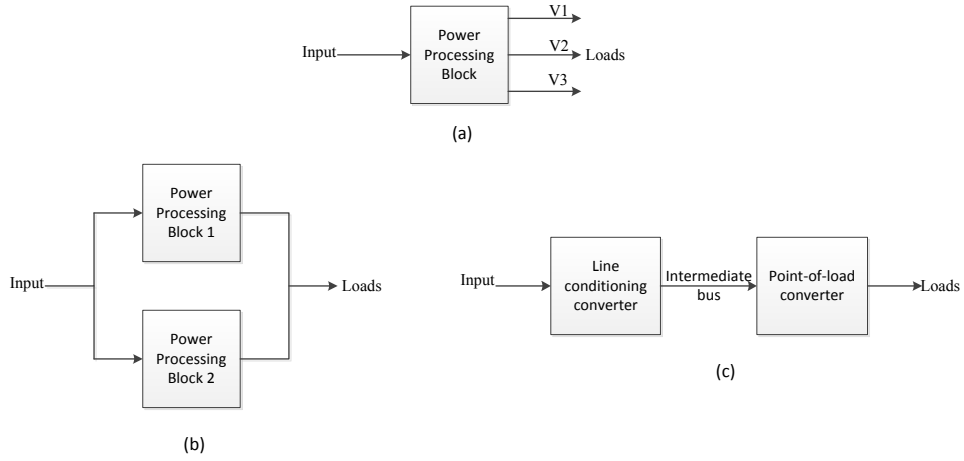


Figure 3: Power distribution architecture (a) Centralized (b) Distributed – parallel configuration (c) Distributed – cascaded configuration.

A cascaded architecture with multiple POL converters is considered here for residential dc distribution system. System configuration based on the location of central ac-dc rectifier and the need for dedicated ac bus is discussed in [3] and [5]. The system studied in [3] discusses European residential distribution while [5] deals with residential systems in Korea. The configurations discussed can be summarized as hybrid ac-dc system and a dc-only system.

2.1.1 Hybrid AC-DC system

As the name suggests this system comprises of both ac and dc buses. AC loads can be connected to the ac bus and dc loads to the dc bus as shown in Figure 4. Such a configuration makes use of the advantages offered by the dc-only and ac-only systems. The disadvantage of using this configuration is two separate bus bars are needed, increasing cost and complexity. The increased complexity may affect availability and operation [11].

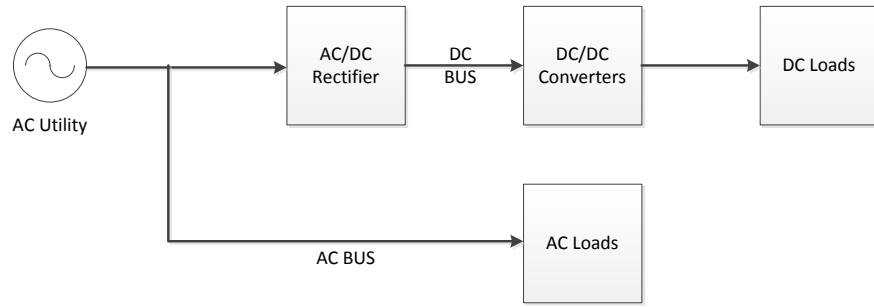


Figure 4: Hybrid AC-DC distribution system.

2.1.2 DC-only system

The results from [5] show a dc-only system with dc transmission by the grid has highest efficiency followed by dc system with ac transmission. The second case with grid-supplied ac power is considered in this work. A central ac-dc rectifier is used to provide the required dc voltage as shown in Figure 5. The voltage levels are discussed later in this chapter. From a system perspective it is observed that this configuration is complementary to the one shown in Figure 1 – the existing ac system. Instead of using multiple ac-dc rectifiers, dc-ac inverters are used for powering ac loads. Since it is assumed that the number of ac loads in a house is lesser than electronic loads and will keep decreasing in near future use of dc-only system can be justified.

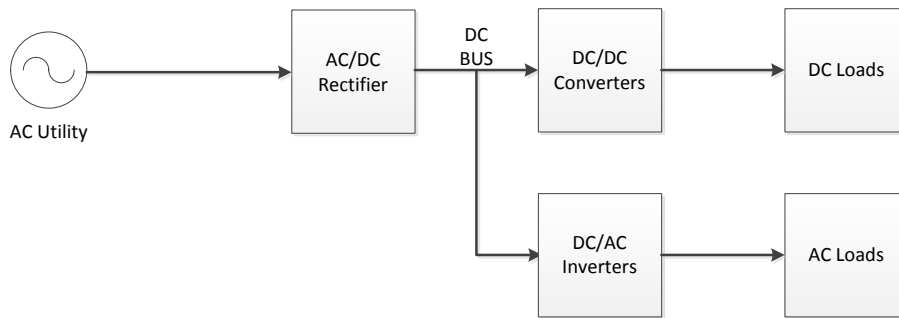


Figure 5: DC distribution system.

The dc-only system is considered in this thesis. The central high power ac-dc rectifier is not considered in system studies but is identified an important component of such a distribution system. As shown in [5] the light load efficiency of central rectifier plays a crucial role in improving the overall system efficiency.

2.2 VOLTAGE SPECIFICATIONS AND SAFETY CONSIDERATIONS

2.2.1 Voltage specification

One of the major hurdles in wide spread adoption of residential level dc system is lack of standard voltage specifications. The existing residential ac voltage standard of single-phase 120V and split-phase 240V in the United States and single-phase 220V and three-phase 380V in Europe has evolved over the years. It is natural that the dc voltage standard will also evolve over the next few years as more research is being conducted in residential dc distribution systems. Literature studied suggests numerous voltage levels based on system requirements and geographical location. The voltage levels are discussed in this section.

A feasibility analysis of four different voltage levels – 325V, 230V, 120V and 48V was conducted in [3]. Results indicate 325V is suitable for residential distribution over longer wire lengths. Low voltages would require lesser protection but losses become too high to use these voltages over long distances. Few studies done in Europe suggest 325V as the bus voltage level [12], [13]. In Europe, ETSI has developed a standard, ETSI EN 300 132-3, for dc and ac powered telecommunications and datacom equipment up to 400V [14]. IEC is currently working on standardization of low voltage dc (LVDC) distribution systems up to 1500V dc [15]. Voltages around 400V dc are being studied as part of this standardization process [16]. In two different studies done in Korea, [5] and [17], 380V was used as the central dc bus voltage level. In US EMerge Alliance, an

alliance of industry and research institute members, has developed a 24V dc standard for occupied space and 380V dc for data center and building services is under development [18], [19]. In [2] two different bus voltages – 380V and 48V were suggested for a dc nanogrid. 380V is used because the existing consumer electronics have an intermediate 380V bus thus rectifier and PFC stage can be bypassed. 48V is considered safe for low power electronic loads and is an existing telecom standard. In [6] simulation studies were performed for a residential dc distribution system using a 48V bus. In [20] six aspects are considered to evaluate appropriate bus voltage level for telecom power architecture. Different voltages were evaluated based on efficiency, energy storage integration, component reliability, safety, cost and flexibility. In general higher voltage tends to improve efficiency, lower conductor cost and is easier to interface with the grid. Meanwhile lower voltage enable easier energy storage integration, improved reliability and are generally safer. It is clear that no single voltage can satisfy all the needs and a trade-off is required.

In this work 380V is chosen as the dc bus voltage for residential distribution. The choice is influenced by the presence of intermediate 380V bus in modern consumer electronic loads and efficiency gains of using a higher voltage level. It is being considered as a standard for residential and commercial locations by IEC [15] and by EMerge Alliance in the US [18]. Considering the current and estimated rate of growth, residential photovoltaic and electric and plug-in hybrid electric vehicles are expected to be common DERs in US residences in near future [8], [21]. 380V dc is compatible with photovoltaic power systems [22] and is also being developed as a standard voltage for fast charging of electric vehicles by SAE International [23] and CHAdeMO, an association of 332 industrial members with interests in electric vehicles [24].

2.2.2 Fault detection and safety issues

In [11] fault detection and mitigation is identified as an issue with dc distributed power architecture. Due to output current limits of power electronic converters a fault cannot be distinguished from full load operation by the upstream line conditioning converters (LCC). Sizing the output capacitor based on energy required to trip the protection device is a simple way to detect and clear faults in distributed power architectures [11]. Another way is to use active protection devices which are built-in the converter. In [2] the idea of controlled converters is suggested which are capable of current monitoring so built-in overcurrent, overvoltage protection can be realized. This reduces the number of slower electromechanical protection devices. However to realize the full functionality of such a controller, communication protocols need to be used that help communicate the status between two converters. This can be advantageous in implementing home energy management systems [25]. Until active protection systems are realized, the traditional electromechanical protection devices need to be used. In [3] it is shown existing ac low voltage circuit breakers can be used in dc circuits however, the ratings should be scaled for a dc current.

In [26] open series fault are compared in ac and dc microgrids. Open series faults may occur due to uncontrollable factors like aging, mechanical stress etc. and under controllable conditions like fuses and circuit breakers. The results from [26] show ac arcs are extinguished faster than dc. However very high transient voltage overshoots, 2-3 times the rated voltage, are observed under ac conditions. DC arcs persist for longer times (50 μ s compared to 5 μ s for ac under constant velocity opening of the connectors) but no voltage transient overshoots are observed. The absence of voltage overshoots in dc systems favors the use of dc in a system with downstream power electronic converters. This is because the transients during fault clearance can damage the components (e.g.

MOSFETs, electrolytic capacitors) in downstream converters. The longer duration arcs in dc conditions result in higher mechanical stresses in the contacts. To make the system reliable and safe, the contact life should be improved when used in dc systems.

The issues of arcing, overvoltage protection, grounding and other protective measures for hazards of dc distribution are being addressed by IEC standards group for LVDC distribution [16].

2.3 CHARACTERIZATION OF DOMESTIC ELECTRIC LOADS

The nature of loads is an important feature that must be studied while designing point-of-load converters in a distribution system. One of the features of dc distribution is independent and optimal design of individual load converters thus improving the overall system efficiency. The steady-state analysis, dynamic performance and ripple requirement of domestic loads are some of the characteristics that need to be studied while designing these converters.

With growing interest in residential dc distribution, there are a few commercially available dc appliances – appliances that are marketed to take a dc input. Some of these are surveyed in [21]. Here, however, existing domestic electric loads are studied and potential future dc appliances are not considered. The existing loads are characterized based on the impedance and power factor they present to the source. A survey of common domestic loads is summarized in Table 1.

2.3.1 Resistive or heating loads

Heating loads are resistive loads and present constant impedance to the source. These are basically used for heating air, water. When switching to a dc system no major change is required as only power rating is important. These loads do not require high dynamic performance and the ripple requirement is not stringent. Power consumption is

from 500W to 1.5kW. The loads can be modeled as a simple resistor based on their power rating. This simple resistive model is used later in this work to design point-of-load converters for heating applications. Examples are toaster, coffee maker, electric heating equipment, incandescent lamps etc. Incandescent bulbs have some dependence of resistor on the input voltage [27].

Table 1: A few common residential loads.

Nature	Loads	Power Rating (W)
Resistive or Heating	Toaster	500-800
	Coffee Maker	1000-1500
	Incandescent bulb	5-200
Inductive or Motor	Fans	10-50
	Washing machine	1000-2000
	Dish washer	1000-2000
	Vacuum cleaner	1000-2000
Constant Power or Electronic	Laptop	50-100
	Desktop computer	100-200
	Lights with electronic ballast and LED lights	20-100
	Chargers for consumer electronics	5-10
	Television sets	150-250

2.3.2 Inductive or motor loads

Induction motors are commonly used in many home appliances. Induction motors in washing machines and dish washers that use variable frequency drives must be interfaced using dc-ac inverter for speed control. The required dynamic performance for

inductive motors can be obtained using the dc-ac inverter. Universal motors in electric fan, vacuum cleaner etc. do not require an inverter and can be directly connected to the dc bus [3]. Motor loads being inductive have a low power factor and in some cases power consumption is higher because of the presence of a high resistor. The interest in dc distribution systems has resulted in growth of dc appliances like air conditioning equipment, refrigerators and fans [21], [28].

2.3.3 Constant power or electronic loads

These are the naturally dc appliances and do not draw much power compared to other two categories. Being dc these loads presently use ac-dc rectifier and have high harmonic content. A power factor correction stage is included to reduce the harmonic distortion. The growing number of such loads is a primary reason to shift towards dc distribution. Some of these appliances would require uninterruptible power supply (UPS) for continued operation. Most of these loads consume constant power [27] and would require better transient performance than previous two categories of loads. The appliances included are all data handling equipment like computers, printers and chargers for portable consumer electronic devices. Lamps with electronic ballasts are also included in this category.

The constant-power loads (CPL) result in stability issues to the main bus. The destabilizing effect arises from negative impedance instability and can cause large voltage oscillations or voltage collapse of the central dc bus [29]. The instantaneous constant-power nature presented by POL converters to the upstream line conditioning converters may destabilize the system as identified in [29]. Solutions based on hardware modifications like adding resistors, filters and energy storage elements to the main bus and load shedding can stabilize the converter at additional cost with lower efficiency. Use

of linear controllers and geometric controllers is more practical without compromising efficiency [29]. The constant-power electronic loads can cause destabilizing effect on the POL converter supplying power to the electronic load. This makes the design of POL converter for electronic loads important from the perspective of system stability. Strategies discussed in [29] should be considered while designing such POL converters.

LED based solid-state lighting has gained significant momentum over the past few years. These lights are dc loads and require power electronic drivers to improve the efficiency and for light dimming. In an ac system these loads require an ac-dc rectifier followed by PFC stage similar to other electronic loads. However in a dc system LED lights can be interfaced using a single POL converter.

For room lighting purposes, LED lamps are arranged in a matrix of series and parallel individual diodes. Depending on the configuration, the voltage requirement is typically 12V – 48V and current is 350mA – 2000mA. The power rating is about 20W - 80W [30].

LEDs behave as a constant voltage source with low equivalent series resistance [31]. An accurate electrical model for the LED around the rated current is shown in Figure 6 [32]. V_{led} is the forward voltage drop of all individual led connected in series. R_{led} is the series resistance. This model is used in simulation studies later in this work.

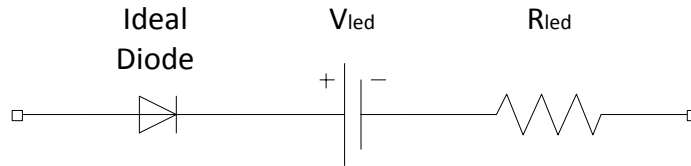


Figure 6: Simple model for LED lighting loads, from [32].

The system configuration, voltage level, safety measures and load characterization were studied in this chapter. The next chapter studies point-of-load converters based on some of the loads discussed here.

Chapter 3: Point-of-load Converters

The residential dc distribution considered here is distributed power system with a central 380V dc bus. In distributed power system architecture, point-of-load converters are located close to loads. The central bus (380V) which is the input bus to POL converters can be loosely regulated whereas the output of POL converters is tightly regulated [10].

In this work the central 380V bus is chosen to have a $\pm 10\%$ regulation. This value of regulation is chosen considering the incorporation of energy storage elements like batteries in future residential dc distribution systems. Although there are a few promising battery technologies like lithium-ion, nickel-cadmium, nickel-metal-hydride etc. low costs and low maintenance requirements make lead-acid batteries the most common choice [21]. Lead-acid battery banks consist of individual battery cells with each cell operating at nominal 2V. These cells are connected in series to obtain desired battery bank voltage based on system requirements. To avoid rapid battery aging due to sulfation of the battery electrode plate, lead-acid batteries should not be discharged below 1.75V and must be kept charged at a float voltage above 2V (around 2.2V) [33]. The battery cell voltage must be kept within $\pm 10\%$ of its nominal value (1.8V – 2.2V). Other battery technologies also have typical minimum and float voltage requirements which would fall within the $\pm 10\%$ variation considered for lead-acid batteries. So the central 380V bus is selected to have $\pm 10\%$ regulation. The wider regulation also simplifies the design of upstream ac-dc rectifier in ac powered grid or upstream dc-dc converters in dc powered grid. On the other hand, the output of POL converter is tightly regulated and generally depends on the load connected at its output. For heating loads the performance is not critical so output is regulated to $\pm 1\%$ under dc conditions.

In most cases the voltage needs to be stepped down and as such buck converters are a natural choice. In cases where low voltages are required like LED lighting (generally $\sim 24V$) transformer coupled topologies will be needed to avoid issues with very low duty cycles. Two converter topologies – a buck converter and a flyback converter are suggested in this chapter. The control for converters is designed and simulation results are presented. Experimental results are discussed in next chapter.

3.1 BUCK CONVERTER

It is the simplest topology to obtain a voltage lower than input voltage. The output voltage level is chosen based on the loads connected. Figure 7 shows the buck converter connected to the dc bus with voltage E and supplying V_{out} to a resistive load. Switches, inductor and capacitor are assumed ideal.

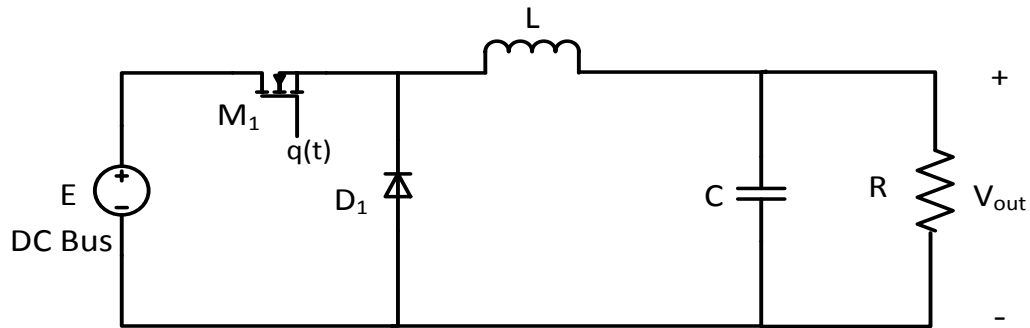


Figure 7: Buck converter.

The MOSFET M_1 is switched on for a specific time (t_{on}) during its switching period (T) during which energy is stored in the inductor. For the remaining period, the diode D_1 conducts and energy stored in inductor is delivered to the load. In steady state the output and input voltage are related by (1). D is the duty cycle.

$$\begin{cases} V_{out} = D \times E \\ D = \frac{t_{on}}{T} \end{cases} \quad (1)$$

3.1.1 Linearized small-signal model of buck converter

Switching converters are non-linear circuits. Various models have been developed to describe the small-signal behavior with linear equations [31]. Such models are useful in designing closed-loop control for the converter. In this section a state space model is developed. Based on this model a state-feedback based control is designed.

Figure 8 (a) shows the configuration of buck converter of Figure 7 when M_1 is on and Figure 8 (b) when M_1 is off. The inductor current, $x_1(t)$, and voltage across the capacitor, $x_2(t)$, are used as the state variables. It is assumed the converter is in continuous conduction mode (CCM) which implies (2).

$$x_1(t) > 0 \quad \forall t > 0 \quad (2)$$

The switching function for M_1 $q(t)$ is defined as follows,

$$q(t) = \begin{cases} 1 & 0 < t \leq t_{on} \\ 0 & t_{on} < t \leq T \end{cases} \quad (3)$$

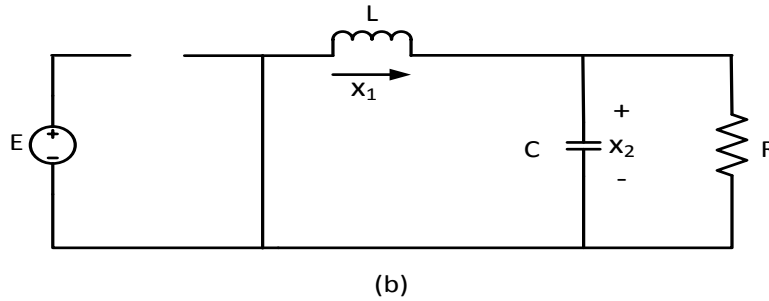
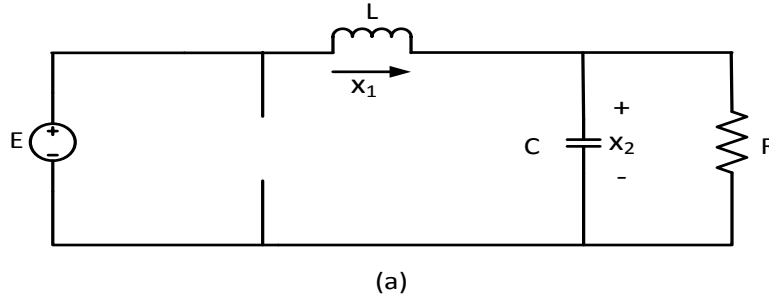


Figure 8: Circuit topology during (a) t_{on} i.e. $q(t) = 1$ and (b) during t_{off} i.e. $q(t) = 0$.

Combining the circuit topologies of Figure 9 and using the switching function $q(t)$, the switched model dynamics for buck converter are shown in (4)

$$\begin{cases} L \frac{dx_1}{dt} = q(t)E - x_2 \\ C \frac{dx_2}{dt} = x_1 - \frac{x_2}{R} \end{cases} \quad (4)$$

$q(t)$ is a non-linear function making (4) a set of non-linear differential equation. A linear operator called fast average operator as defined in (5) can be used to transform the switched equations to average equations shown in (7) [34]. T is the switching period of the converter. The fast average operation on switching function $q(t)$ yields the average switching function $\bar{d}(t)$ as shown in (6)

$$\bar{f}(t) = \frac{1}{T} \int_t^{t+T} f(t) dt \quad (5)$$

$$\bar{d}(t) = \frac{1}{T} \int_t^{t+T} q(t) dt \quad (6)$$

$$\begin{cases} L \frac{d\bar{x}_1}{dt} = \bar{d}(t)E - \bar{x}_2 \\ C \frac{d\bar{x}_2}{dt} = \bar{x}_1 - \frac{\bar{x}_2}{R} \end{cases} \quad (7)$$

In equilibrium the rate of change of state is zero. Thus the equilibrium points can be obtained by equating LHS of (7) to zero and are shown in (8).

$$\begin{cases} \bar{X}_{2e} = D_e E \\ \bar{X}_{1e} = \frac{\bar{X}_{2e}}{R} = \frac{D_e E}{R} \end{cases} \quad (8)$$

Let δx_1 and δx_2 be the small perturbations around the equilibrium points defined in (8). δd and δE are the perturbations in equilibrium duty cycle and the input voltage.

Using these in (7) gives (9)

$$\begin{cases} L \frac{d(\delta x_1 + \bar{X}_{1e})}{dt} = (\bar{d} + D_e)(E + \delta E) - (\bar{x}_2 + \bar{X}_{2e}) \\ C \frac{d(\delta x_2 + \bar{X}_{2e})}{dt} = (\delta x_1 + \bar{X}_{1e}) - \frac{(\delta x_2 + \bar{X}_{2e})}{R} \end{cases} \quad (9)$$

Simplifying (9) and using (8) we have the small signal differential equation given in (10), [34]

$$\begin{cases} L \frac{d\delta\bar{x}_1}{dt} = \delta\bar{d}E + D_e\delta E - \delta\bar{x}_2 \\ C \frac{d\delta\bar{x}_2}{dt} = \delta\bar{x}_1 - \frac{\delta\bar{x}_2}{R} \end{cases} \quad (10)$$

The complete state-space representation of the small signal model is shown in (11). For ideal buck converter the output, δy , is voltage across the capacitor, δx_2 .

$$\begin{cases} \begin{pmatrix} \delta\dot{x}_1 \\ \delta\dot{x}_2 \end{pmatrix} = \begin{pmatrix} 0 & \frac{-1}{L} \\ \frac{1}{C} & \frac{-1}{RC} \end{pmatrix} \begin{pmatrix} \delta x_1 \\ \delta x_2 \end{pmatrix} + \begin{pmatrix} \frac{E}{L} \\ 0 \end{pmatrix} \delta\bar{d} + \begin{pmatrix} \frac{D_e}{L} \\ 0 \end{pmatrix} \delta E \\ \delta y = (0 \quad 1) \begin{pmatrix} \delta x_1 \\ \delta x_2 \end{pmatrix} + \begin{pmatrix} 0 \\ 0 \end{pmatrix} \delta\bar{d} + \begin{pmatrix} 0 \\ 0 \end{pmatrix} \delta E \end{cases} \quad (11)$$

The circuit with non-idealities is shown in Figure 9. The non-idealities included are on-resistance of MOSFET (R_{ON}), dc resistance (DCR, R_{DCR}) of inductor and equivalent series resistance (ESR, R_c) of output capacitor. For simplicity the on-resistance of diode is also assumed to be R_{ON} .

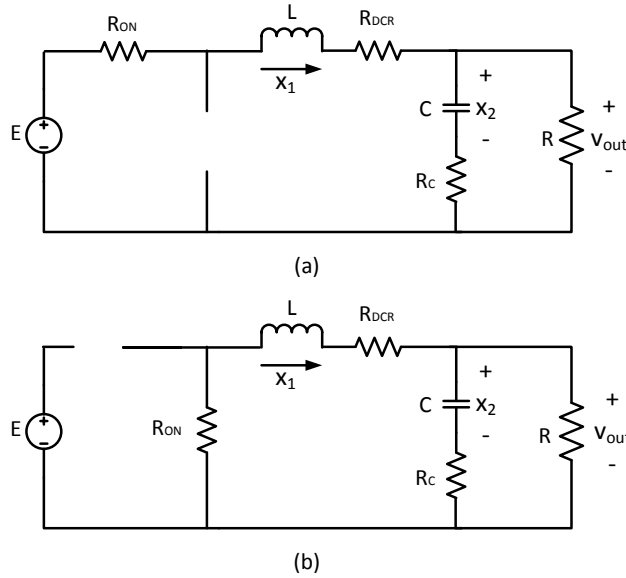


Figure 9: Circuit topology including non-idealities during (a) t_{on} i.e. $q(t) = 1$ and (b) during t_{off} i.e. $q(t) = 0$.

The switched dynamic equations for the circuit of Figure 10 are given in (12)

$$\begin{cases} L \frac{dx_1}{dt} = q(t)E - x_1(R_{ON} + R_{DCR}) - v_{out} \\ C \frac{dx_2}{dt} = x_1 - \frac{v_{out}}{R} \end{cases} \quad (12)$$

The output voltage, v_{out} , is related to the state variables by (13).

$$v_{out} = \frac{R_C R}{R + R_C} x_1 + \frac{R}{R + R_C} x_2 \quad (13)$$

Using (12) and (13), the non-ideal buck converter can be described by (14)

$$\begin{cases} L \frac{dx_1}{dt} = q(t)E - x_1(R_{ON} + R_{DCR} + \frac{R_C R}{R + R_C}) - \frac{R}{R + R_C} x_2 \\ C \frac{dx_2}{dt} = \frac{R}{R + R_C} x_1 - \frac{1}{R + R_C} x_2 \\ y = v_{out} = \frac{R_C R}{R + R_C} x_1 + \frac{R}{R + R_C} x_2 \end{cases} \quad (14)$$

Using the linearization technique used previously for ideal buck converter, the small-signal linear model for non-ideal buck converter is given in (15)

$$\begin{cases} \begin{pmatrix} \delta \dot{x}_1 \\ \delta \dot{x}_2 \end{pmatrix} = \begin{pmatrix} \frac{-1}{L} \left(\frac{R_C R}{R_C + R} + R_{DCR} + R_{ON} \right) & \frac{-1}{L} \left(\frac{R}{R_C + R} \right) \\ \frac{1}{C} \left(\frac{R}{R_C + R} \right) & \frac{-1}{C} \left(\frac{1}{R_C + R} \right) \end{pmatrix} \begin{pmatrix} \delta x_1 \\ \delta x_2 \end{pmatrix} + \begin{pmatrix} \frac{E}{L} \\ 0 \end{pmatrix} \overline{\delta d} + \begin{pmatrix} \frac{D_e}{L} \\ 0 \end{pmatrix} \delta E \\ \delta y = \begin{pmatrix} \frac{R_C R}{R_C + R} & \frac{R}{R_C + R} \end{pmatrix} \begin{pmatrix} \delta x_1 \\ \delta x_2 \end{pmatrix} + \begin{pmatrix} 0 \\ 0 \end{pmatrix} \overline{\delta d} + \begin{pmatrix} 0 \\ 0 \end{pmatrix} \delta E \end{cases} \quad (15)$$

Using this model the open loop response of buck converter is simulated with MATLAB. The output voltage is shown in Figure 10. Parameters used for simulation and experiment are shown in Table 2. Initial simulations were done using a switching frequency of 100 kHz considering a smaller inductance and output capacitor. However experimental verification became difficult at 100 kHz because of transient issues with the MOSFET driver arising from parasitic elements so a lower frequency of 50 kHz was used.

Table 2: Parameters used in simulation of buck converter.

Parameter	Value	Unit
E	380	V
V_{out}	100	V
L	640	μH
C	20	μF
R	20	Ω
f_{sw} (switching frequency)	50	kHz
R_{ON} (MOSFET on resistance)	290	$\text{m}\Omega$
R_{DCR} (Inductor dc resistance)	100	$\text{m}\Omega$
R_C (Capacitor equivalent series resistance)	5	Ω

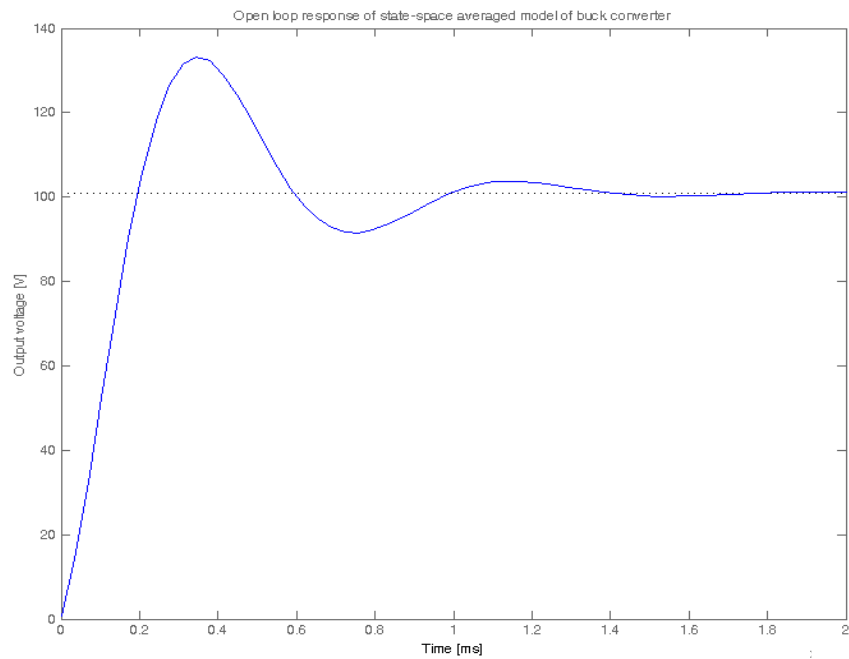


Figure 10: Open loop response of state-space average model.

3.1.2 State feedback control of buck converter

A robust controller can be designed using state-feedback control with reference tracking. Such a controller is robust to disturbances as well as modeling inaccuracies. [35]. In this section a state feedback controller is designed for the linearized model of the buck converter from previous section.

Voltage mode control is a commonly used technique in control of buck converters. In this technique a saw-tooth signal is compared with a reference signal V_{ref} to obtain the duty cycle during each switching period. The perturbation in duty cycle δd is proportional to the perturbation in reference voltage δv_{ref} as shown in (16) where D and V_{ref} are the equilibrium points for duty cycle and reference voltage respectively [31].

$$\delta d = \frac{D}{V_{ref}} \delta v_{ref} \quad (16)$$

Here for simplicity it is assumed there is no perturbation in line voltage i.e. $\delta E = 0$ but will be considered later. Using (15), (14) can be simplified to,

$$\begin{cases} \begin{pmatrix} \delta \dot{x}_1 \\ \delta \dot{x}_2 \end{pmatrix} = \begin{pmatrix} \frac{-1}{L} \left(\frac{R_C R}{R_C + R} + R_{DCR} + R_{ON} \right) & \frac{-1}{L} \left(\frac{R}{R_C + R} \right) \\ \frac{1}{C} \left(\frac{R}{R_C + R} \right) & \frac{-1}{C} \left(\frac{1}{R_C + R} \right) \end{pmatrix} \begin{pmatrix} \delta x_1 \\ \delta x_2 \end{pmatrix} + \begin{pmatrix} \frac{E}{L} \\ 0 \end{pmatrix} \frac{D}{V_{ref}} \delta v_{ref} \\ \delta y = \begin{pmatrix} \frac{R_C R}{R_C + R} & \frac{R}{R_C + R} \end{pmatrix} \begin{pmatrix} \delta x_1 \\ \delta x_2 \end{pmatrix} + \begin{pmatrix} 0 \\ 0 \end{pmatrix} \frac{D}{V_{ref}} \delta v_{ref} \end{cases} \quad (17)$$

The states are inductor current and capacitor voltage. Input to the system is δv_{ref} . (18) is the short hand notation for (17)

$$\begin{cases} \delta \dot{x} = A \delta x + B \delta v_{ref} \\ \delta y = C \delta x + D \delta v_{ref} \end{cases} \quad (18)$$

A full state feedback controller with arbitrary pole locations can be designed if the system is controllable [36]. In this case the rank of controllability matrix (=2) is same as the number of states (=2) so the system is controllable. Thus the system described in (17) can be controlled using full state feedback shown in (19)

$$\begin{cases} \delta v_{ref} = -K \begin{pmatrix} \delta x_1 \\ \delta x_2 \end{pmatrix} \\ K = \begin{pmatrix} k_1 & k_2 \end{pmatrix} \end{cases} \quad (19)$$

Applying state feedback to (18) gives,

$$\begin{cases} \delta \dot{x} = (A - BK) \delta x \\ \delta y = C \delta x \end{cases} \quad (20)$$

The closed loop poles of (20) are based on the elements of K . Thus a desired response can be obtained by using pole placement technique. The closed loop system is shown in Figure 11 and the output response is shown in Figure 12 (a). A simple state feedback control is basically a proportional control and leads to a steady-state error as shown in Figure 12.

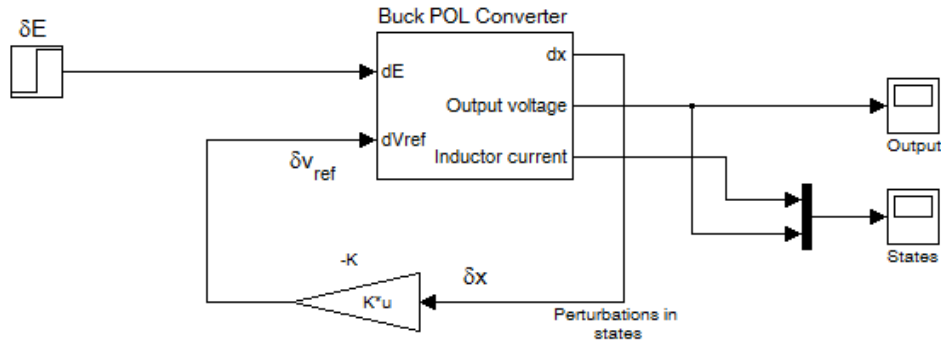


Figure 11: State-feedback control of buck converter.

To achieve zero steady-state error and to make the system immune to changes in input voltage and other disturbances, an integral control is needed. The integral control is designed based on the method discussed in [37]. In this method the error between reference output and the actual output is used as a new state p as defined in (21). Y is the equilibrium point of output voltage and Y_{ref} is the output reference voltage. Both are the same quantities so p is the integral of perturbation in output voltage.

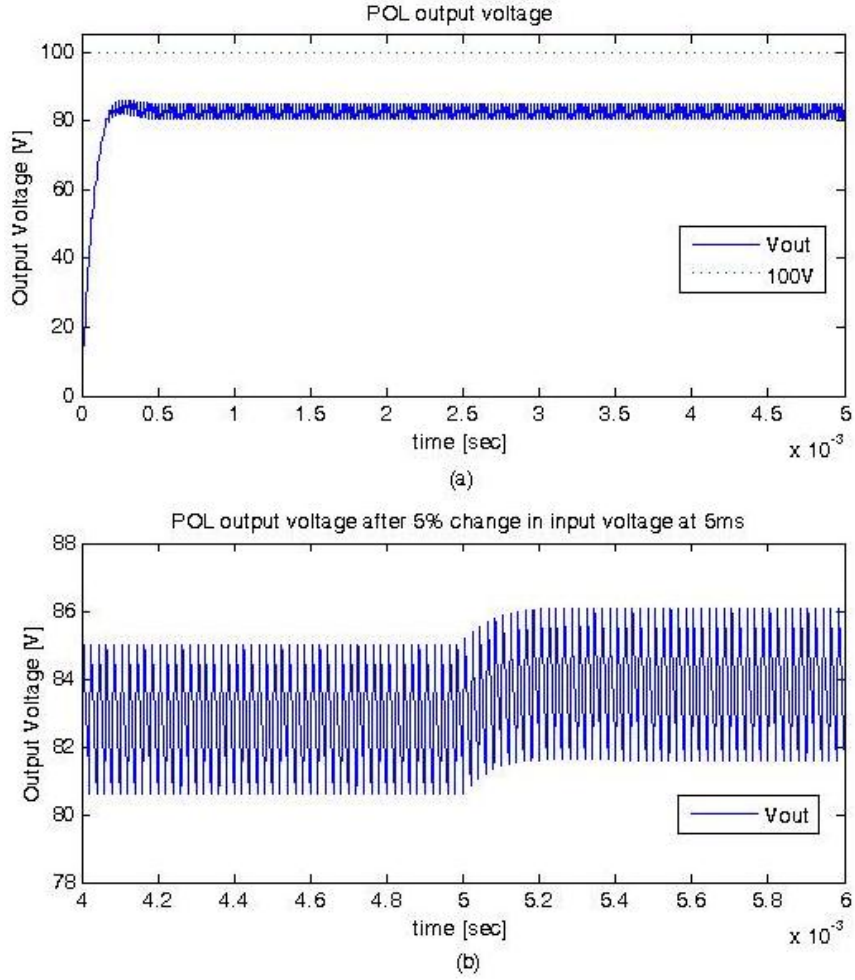


Figure 12: Circuit simulation of closed loop buck converter (a) output voltage with steady-state error (b) output voltage with a 5% step change in input voltage.

$$\begin{cases} p = \int_0^t ((Y + \delta y) - Y_{ref}) dt \\ p = \int_0^t (\delta y) dt \end{cases} \quad (21)$$

Including the change in input voltage δE as a disturbance input, (18) can be written as,

$$\begin{cases} \delta \dot{x} = A \delta x + B \delta v_{ref} + B' \delta E \\ \dot{p} = \delta y = C \delta x + D \delta v_{ref} \end{cases} \quad (22)$$

In matrix form,

$$\dot{z} = \begin{pmatrix} \dot{\delta x} \\ \dot{p} \end{pmatrix} = \begin{pmatrix} A & 0 \\ C & 0 \end{pmatrix} \begin{pmatrix} \delta x \\ p \end{pmatrix} + \begin{pmatrix} B \\ D \end{pmatrix} \delta v_{ref} + \begin{pmatrix} B' \\ 0 \end{pmatrix} \delta E \quad (23)$$

In steady-state, $\dot{\delta x} = 0$ and $\dot{p} = 0$

$$\begin{pmatrix} B' \\ 0 \end{pmatrix} \delta E = - \begin{pmatrix} A & 0 \\ C & 0 \end{pmatrix} \begin{pmatrix} \delta x_s \\ p_s \end{pmatrix} - \begin{pmatrix} B \\ D \end{pmatrix} \delta v_{ref_s} \quad (24)$$

Let the deviation from the steady state be defined as,

$$\begin{cases} z = \begin{pmatrix} \delta x - \delta x_s \\ p - p_s \end{pmatrix} \\ \dot{z} = \begin{pmatrix} \dot{\delta x} \\ \dot{p} \end{pmatrix} \\ v = \delta v_{ref} - \delta v_{ref_s} \end{cases} \quad (25)$$

Using (24) and (25) gives,

$$\begin{cases} \dot{z} = \hat{A}z + \hat{B}v \\ \hat{A} = \begin{pmatrix} A & 0 \\ C & 0 \end{pmatrix} \\ \hat{B} = \begin{pmatrix} B \\ D \end{pmatrix} \end{cases} \quad (26)$$

(26) is similar to (18) with a new state z . Again a row vector of constant gains K can be designed using pole placement technique to obtain the desired response. In (27) K has as many elements as states and can be partitioned in K_1 and K_2 . K_1 is a row vector of two elements corresponding to the feedback gains of two states and K_2 is the gain of the integral of output perturbation.

$$\begin{cases} v = -Kz \\ \delta v_{ref} - \delta v_{ref_s} = -K_1(\delta x - \delta x_s) - K_2(p - p_s) \\ \delta v_{ref} = -K_1(\delta x) - K_2 \int_0^t (\delta y) dt \end{cases} \quad (27)$$

Thus a proportional state feedback with integral control is designed. The closed loop system with integral control is shown in Figure 13.

As suggested in [36] closed loop poles can be selected as the poles of the Bessel filter of the same order. This is because step response of such a filter does not have an

overshoot. So the poles can be selected based on the desired settling time. Using the 3rd order Bessel filter and a settling time of 0.24msec the pole locations are $\{-1.9721e4, -1.5617e4 \pm i1.4899e4\}$. The MATLAB *place* command is used to generate the gain vector K. The simulation results of buck converter with state feedback and integral control are shown in Figure 14.

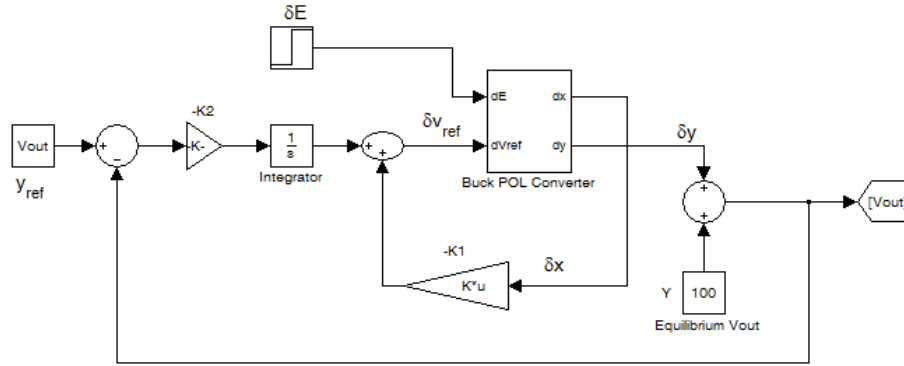
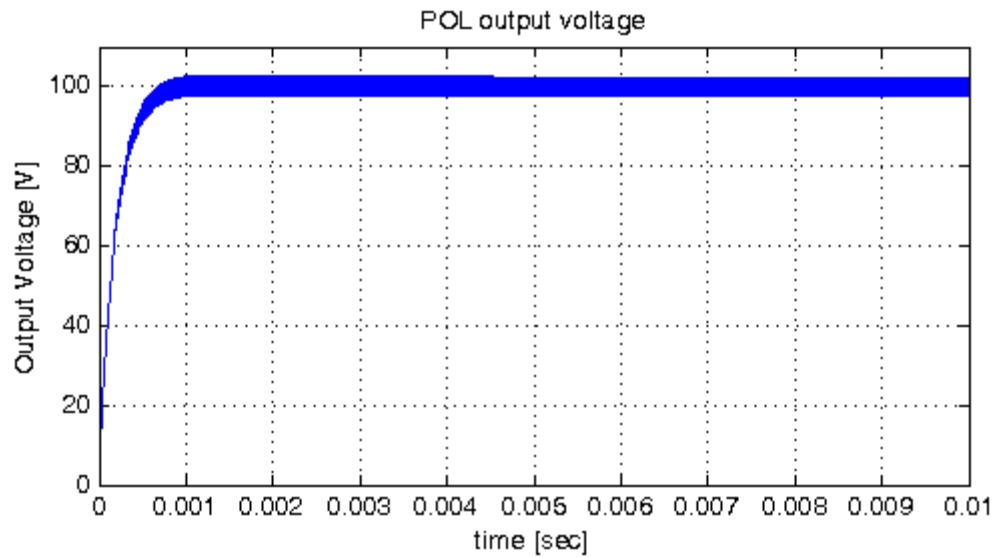


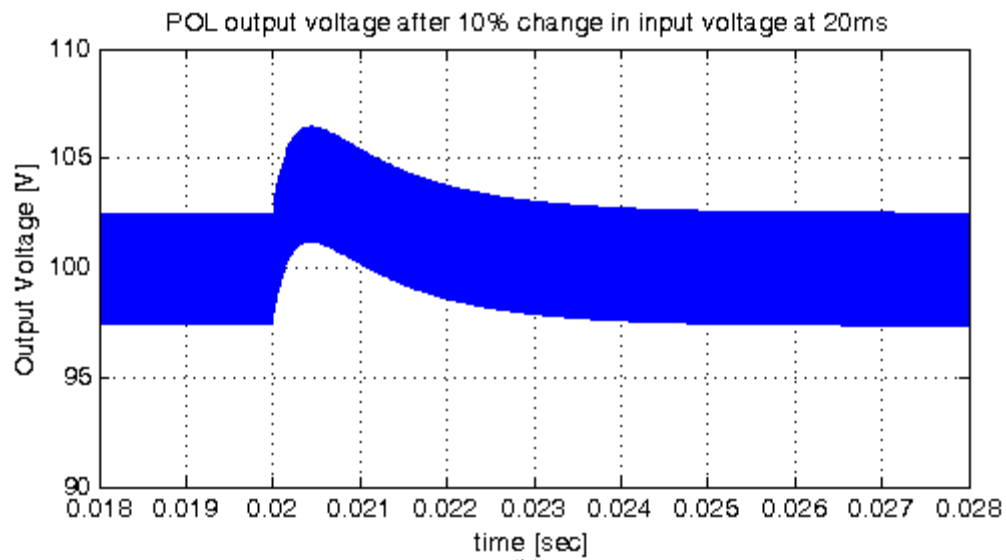
Figure 13: State-feedback with integral control of buck converter.

As seen in Figure 14, there is no steady-state error in the output voltage. Also the output voltage settles to 100V after a 10% step change in the input. A feed-forward gain from V_{ref} is added to improve the transient performance. Compared to the open loop response of Figure 10, no overshoot in the output voltage is seen in Figure 14.

Such a buck converter can be used as POL converter to provide different voltage levels. Since the inductor current is used as a state variable the load current can be monitored and appropriate over current protection features can be incorporated using this control technique. As discussed in section 2.3.1 heating loads can work satisfactorily when they are powered by dc voltage equal to the RMS value of existing ac voltage. In the next chapter, experimental results for a buck converter implemented as a POL converter for heating loads are presented.



(a)



(b)

Figure 14: Circuit simulation of closed loop buck converter with integral control (a) output voltage without steady-state error (b) output voltage with a 10% step change in input voltage.

3.2 FLYBACK CONVERTER

3.2.1 LED drivers

LED based solid state lighting (SSL) in ambient illumination is increasing due to the benefits of higher efficiency and longer life-times [31]. LEDs are commonly arranged in matrix of parallel and series connected diodes. Usually these are operated at low voltages (12V – 48V) [30]. Using a buck converter in this case would require a very low duty cycle for example to obtain 24V output from a 380V bus, the duty cycle needs to be 6.3%. Lower duty cycle compromises the efficiency and in cases where higher switching frequency is used requires fast switching MOSFET which increases the cost. So isolated converter topology is preferred POL converter for LED lighting loads in residential dc distribution system.

The effect of output current waveform on luminous efficiency of LEDs is discussed in [38]. The results show highest efficiency is achieved when the LED current is pure dc. DC current superimposed with a small ripple yield similar performance. Thus pulse width modulated converters are a good choice to drive LED loads.

In [39] it is suggested that to keep the driver cost low and to extend the driver life-time the output capacitor used in power converters should be removed. These reasons, although compelling, do not justify the loss in efficiency caused by pulsating nature of LED current.

Flyback converter is a commonly used transformer coupled topology. It is very efficient for power levels below 100W [39]. The flyback converter is suggested as the POL converter for LED lighting loads. The converter and its control are discussed in the next section.

3.2.2 Flyback as POL converter for LED lighting loads

Figure 15 shows a typical flyback converter. The topology is derived from the buck-boost converter. The magnetic device, T , shown as a transformer in Figure 16 is not an actual transformer but two coupled inductors. The device is sometimes referred to as the flyback transformer. Unlike the ideal transformer, current does not flow simultaneously in both the windings. When M_1 is on energy is stored in the first winding. This puts D_1 in reverse bias and does not conduct. The energy stored in output capacitor is transferred to the load during this period. When M_1 is off, to maintain constant magnetic flux in the coupled inductors, the voltage across the windings reverses polarity. Thus D_1 is now forward biased and the energy from the coupled inductors is transferred to the load and output capacitor.

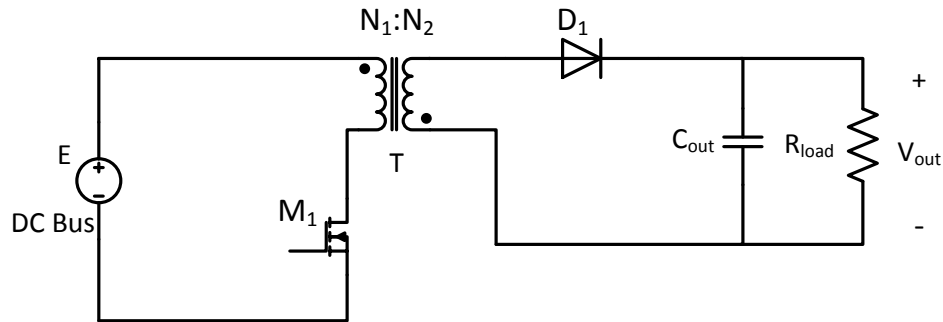


Figure 15: Flyback converter.

A state-space model of the flyback converter is developed. In this analysis, the flyback transformer can be modeled as an ideal transformer with same turns ratio in parallel with magnetizing inductance (L_M) as shown in Figure 16 (a) [40]. The turns ratio for the ideal transformer is $N_1:N_2 = 1:n$. The state variables are current through L_M called the magnetizing current, x_1 , and voltage across the output capacitor, x_2 . The switching

function $q(t)$ that is used to control M_1 is same as defined in (3). The circuit elements are considered ideal in this analysis.

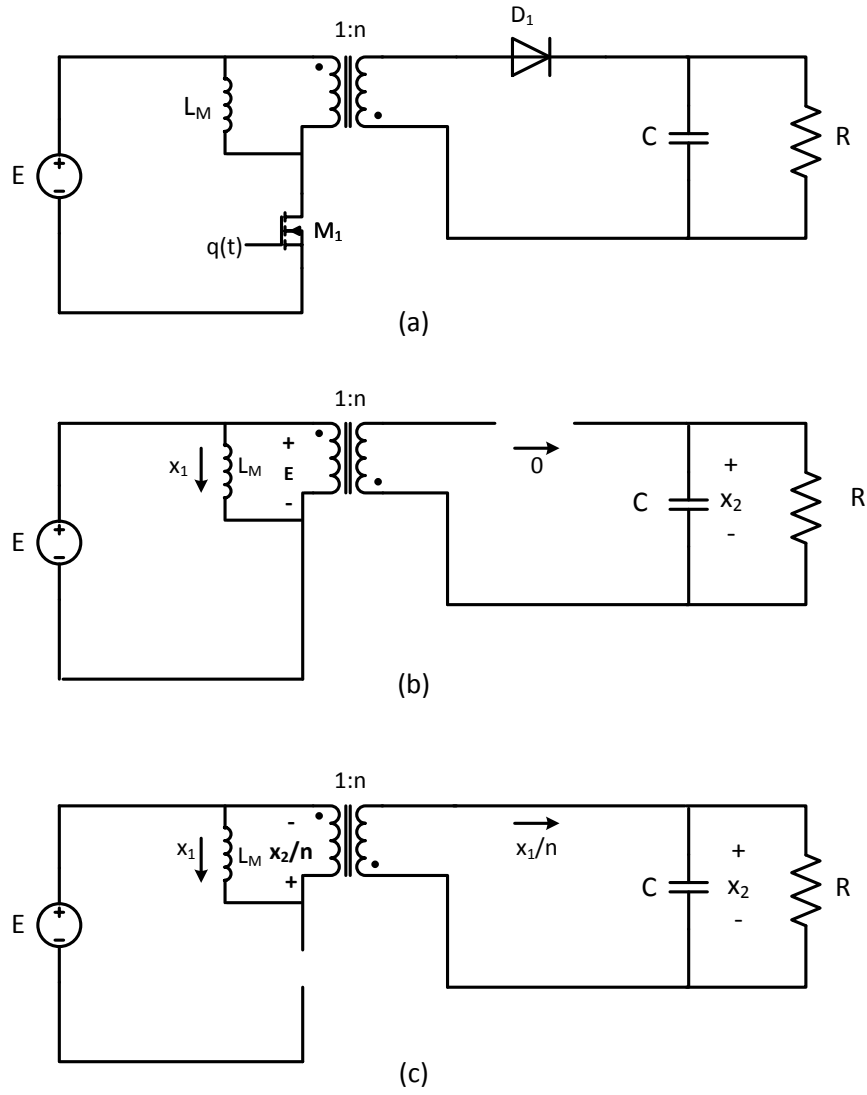


Figure 16: Flyback converter (a) with transformer equivalent circuit (b) when $q(t)=1$ (c) when $q(t)=0$.

The dynamic equations describing the circuit in Figure 16 (b) and (c) are shown in (28) and (29) respectively.

$$\begin{cases} L_M \frac{dx_1}{dt} = E \\ C \frac{dx_2}{dt} = -\frac{x_2}{R} \end{cases} \quad (28)$$

$$\begin{cases} L_M \frac{dx_1}{dt} = -\frac{x_2}{n} \\ C \frac{dx_2}{dt} = \frac{x_1}{n} - \frac{x_2}{R} \end{cases} \quad (29)$$

Using the switching function the above equations can be combined to give (30) where $q'(t) = 1 - q(t)$

$$\begin{cases} L_M \frac{dx_1}{dt} = q(t)E - q'(t)\frac{x_2}{n} \\ C \frac{dx_2}{dt} = q'(t)\frac{x_1}{n} - \frac{x_2}{R} \end{cases} \quad (30)$$

The approach used to obtain the small-signal model of buck converter can be used to obtain the small-signal model of the flyback converter shown in (31). The average steady-state operating points for the converter are shown in (32).

$$\begin{cases} \begin{pmatrix} \delta \dot{x}_1 \\ \delta \dot{x}_2 \end{pmatrix} = \begin{pmatrix} 0 & \frac{-D'}{nL_M} \\ \frac{D'}{nC} & \frac{-1}{RC} \end{pmatrix} \begin{pmatrix} \delta x_1 \\ \delta x_2 \end{pmatrix} + \begin{pmatrix} \frac{1}{L_M} (E + \frac{\bar{X}_{2e}}{n}) \\ -\frac{\bar{X}_{1e}}{nC} \end{pmatrix} \bar{\delta d} + \begin{pmatrix} \frac{D}{L} \\ 0 \end{pmatrix} \delta E \\ \delta y = (0 \quad 1) \begin{pmatrix} \delta x_1 \\ \delta x_2 \end{pmatrix} + \begin{pmatrix} 0 \\ 0 \end{pmatrix} \bar{\delta d} + \begin{pmatrix} 0 \\ 0 \end{pmatrix} \delta E \end{cases} \quad (31)$$

$$\begin{cases} \bar{X}_{2e} = \frac{D}{D'} nE \\ \bar{X}_{1e} = \frac{n\bar{X}_{2e}}{D'R} \end{cases} \quad (32)$$

The open loop circuit response is shown in Figure 17. The parameters used in simulation are summarized in Table 3. LED drivers are usually designed to have a smaller size with drivers located behind the LED strings to keep the thickness of LED lamp minimum [38]. To reduce the size of driver, higher switching frequency of 100 kHz is used in the simulation. The LED equivalent model shown in Figure 6 is used as the load for this simulation. The simulation is performed using SimPowerSystems tool from MATLAB and the circuit shown in Figure 16 (a) is used.

Table 3: Parameters used in simulation of flyback converter.

Parameter	Value	Unit
E	380	V
V_{out}	24	V
L_M	2400	μH
C	32	μF
R_{LED}	0.8	Ω
V_{LED}	24	V
f_{sw} (switching frequency)	100	kHz
n (turns ratio of flyback transformer)	36/380	-
D (duty cycle)	40	%
R_{ON} (MOSFET on resistance)	290	m Ω

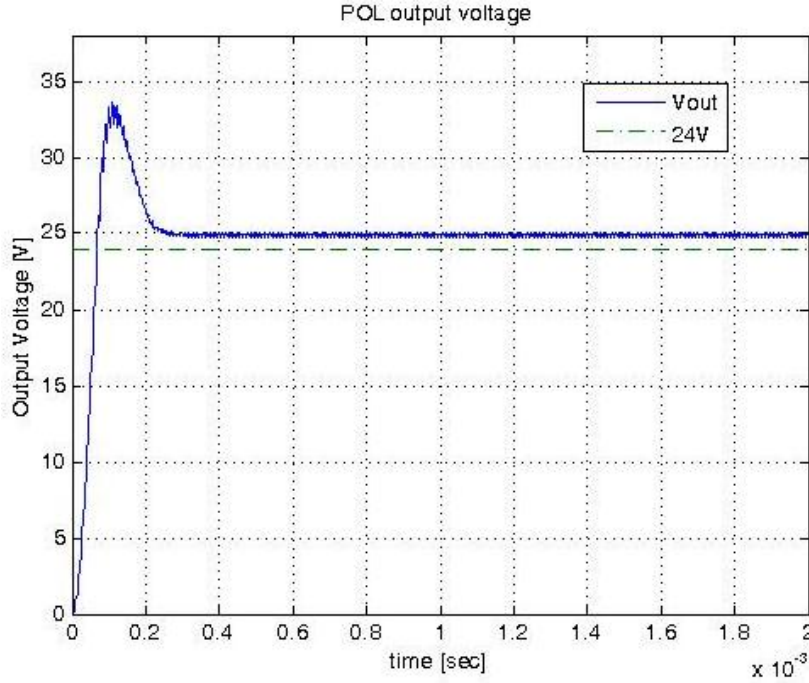


Figure 17: Open loop response of flyback converter.

The first state variable for this converter namely the magnetizing current is not physically measurable. This makes the use of state-feedback technique complicated for the flyback converter. However control of flyback converter is widely studied topic [31], [40], [41] and there exist commercially available ICs to serve this purpose. As discussed in section 3.2.1 current mode control is preferred control technique for converters used as drivers for LED loads. There are numerous studies [32], [39], [42] and [43] demonstrating the use of current controlled flyback converter as a LED driver. In all cases the input to the flyback was rectified line voltage. In this work the flyback converter is connected to the high voltage dc bus.

Peak current mode control (PCMC) of flyback converter has problems like poor noise immunity, lesser accuracy and sub-harmonic oscillations for duty ratio greater than 0.5 [41]. Also for a flyback converter using PCMC, the inductor current is controlled

which is not the same as output current. Average current model control (ACMC) overcomes the problems of PCMC and can control the output current of the flyback converter [40]. The ACMC of flyback converter is shown in Figure 18. Here, G and H are the sensor gains for current and voltage respectively.

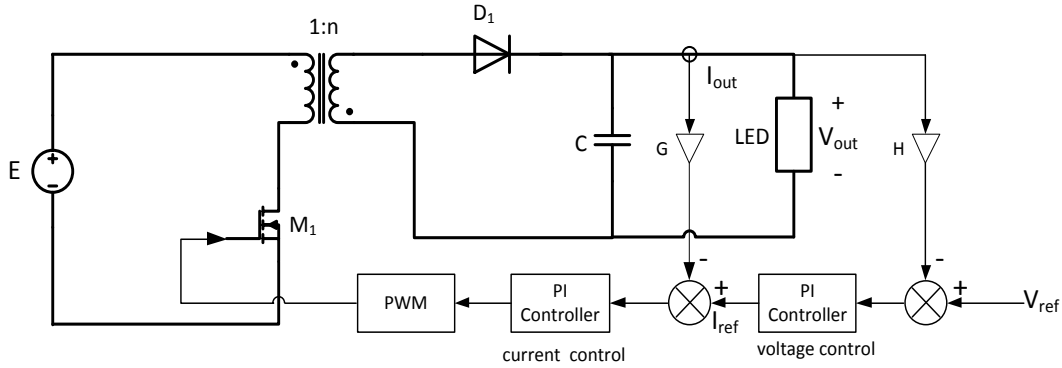


Figure 18: Average current mode control of flyback converter.

The outer voltage loop tracks the changes in output voltage and is used to generate a current reference I_{ref} to control the output current. Both the voltage and current controller are generic PI control. The load used is the equivalent model for LED with V_{LED} and R_{LED} parameters shown in Table 3.

The closed loop response of the converter is shown in Figure 19. As seen in the figure the output voltage has very low ripple as the LED load acts as a constant voltage load. Thus the output capacitor can be reduced or completely removed. However, the capacitor also keeps the output current ripple to a low value which is important for efficient performance of the LED. The output current is 0 initially because of the ideal diode used in the equivalent model of LED. Once the output voltage reaches 24V, current starts to increase. Output current has a ripple of $\sim 180\text{mA}$.

In this chapter, two basic converter topologies were suggested as POL converters for heating and LED lighting loads. Their control was discussed and simulation results were presented. These converter simulation models are used in simulation of a residential dc distribution system. The next chapter presents experimental results of the closed-loop buck converter for heating loads.

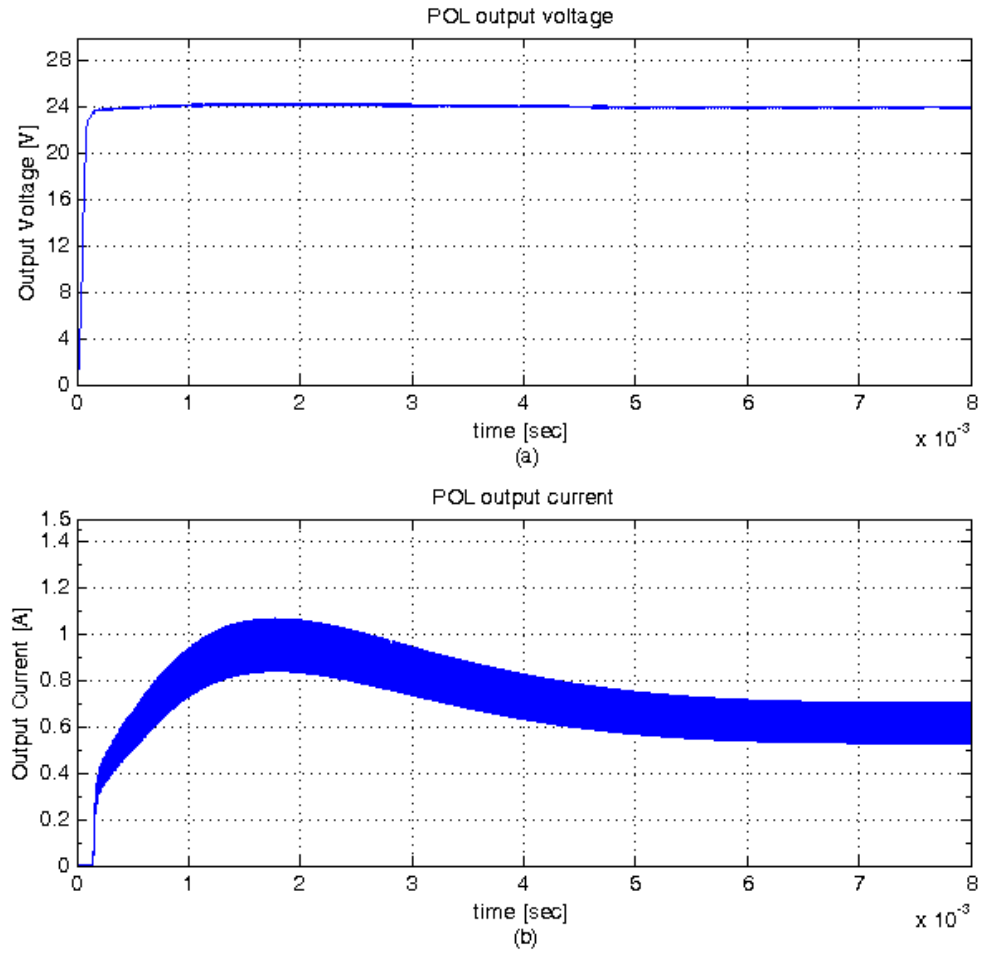


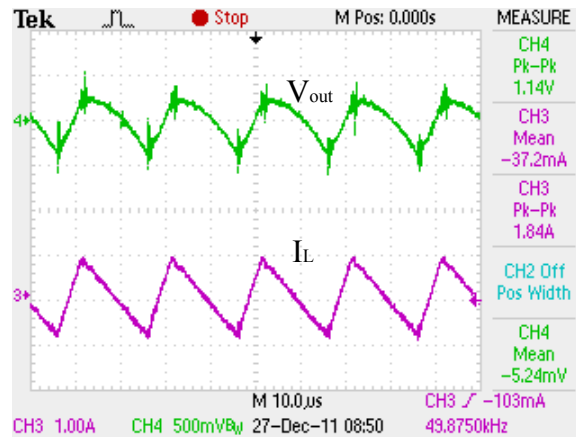
Figure 19: Closed loop flyback (a) output voltage (b) output current.

Chapter 4: Experimental Results of POL Buck Converter

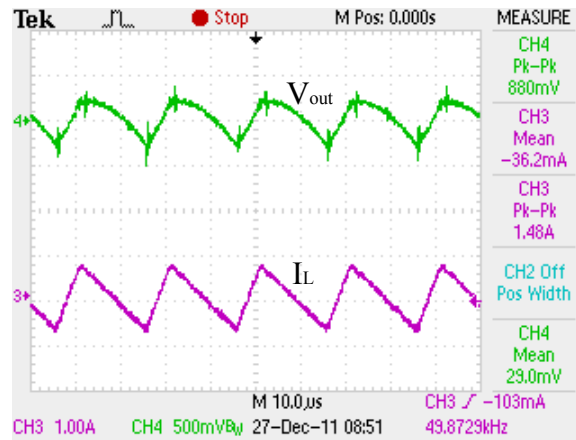
The buck converter control discussed in section 3.1.2 is implemented as a POL converter for heating loads. Domestic heating loads are usually rated in the range of 500W – 1500W. Here, a 500W buck converter is designed for heating loads. The results are discussed in this chapter.

The 380V dc bus is simulated using Magna-power electronics XR series dc power supply. The output voltage level selected is 100V. The converter parameters are shown in Table 2. The inductor is designed using toroidal core T300-26D from Micrometals. High voltage N-channel MOSFET 17N80C3 from Infineon is selected as it has low on-resistance. IRS2110 is used to drive the MOSFET. RHRP1560 diode is used for the freewheeling diode in buck converter and also for bootstrapping circuit of the driver. The resistive load is simulated using programmable electronic load – Chroma 63804. Two electrolytic capacitors in parallel, each with an ESR of 9.4Ω at 100Hz, are used as output capacitors. Op-amps LM258 are used as buffers, gain amplifiers for state-feedback gains and for integral control. ICL8038 is used to generate the reference waveform and comparator LM393 is used to generate the PWM input signal for MOSFET driver. A $10m\Omega$ shunt resistor is used to measure the inductor current.

Figure 20 shows the ripple in output voltage (V_{out}) and inductor current (I_L) at full load and half load. At rated load current, the ripple in output voltage is about 1% of the output voltage while inductor current has ripple of 1.84A (~37% of rated load current).



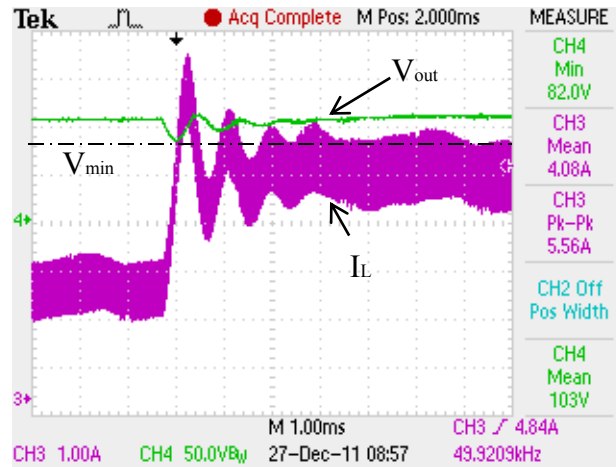
(a)



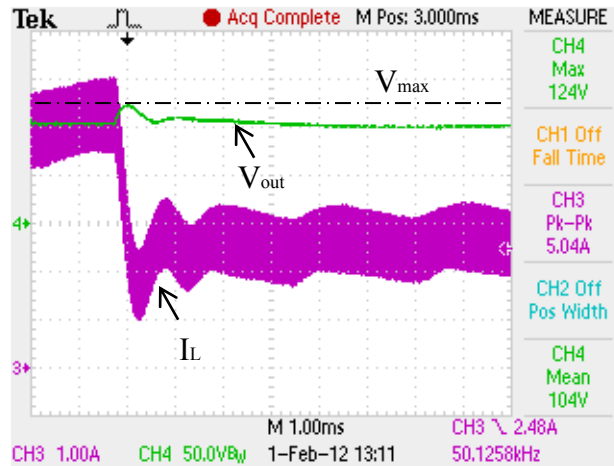
(b)

Figure 20: Ripple in output voltage and inductor current when load current is (a) 5A (b) 2.5A.

Figure 21 shows the response of the converter to load changes. When load increases from 2.5A to 5A, undershoot of 18V is seen in the output voltage and output settles to 100V in 5ms. On load release of equal magnitude overshoot of 24V is seen with output settling to 100V in 5ms. The transient performance is not critical for heating loads and the response observed here should be satisfactory.



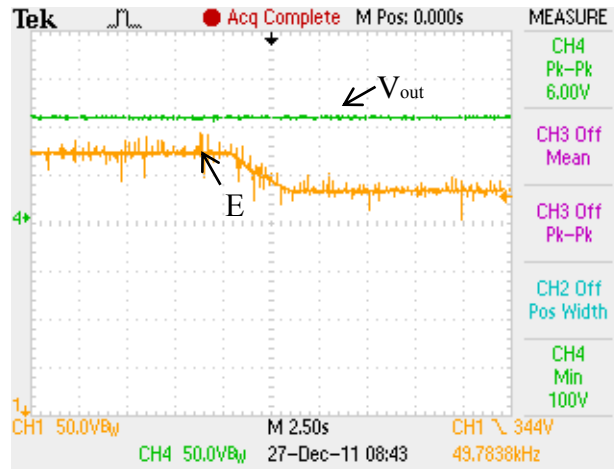
(a)



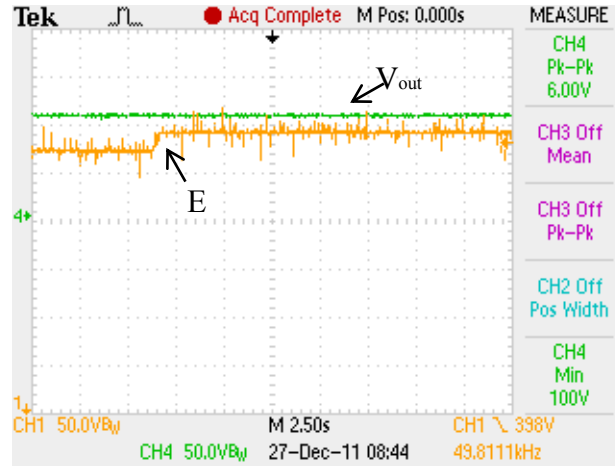
(b)

Figure 21: Response of converter due to step change in output current (a) from 2.5A to 5A (b) from 5A to 2.5A.

Line regulation is important for POL converters because the central dc bus is allowed to have wider voltage variations. The simulations showed stable behavior for $\pm 10\%$ change in input voltage. Figure 22 shows line regulation of the converter for -10% and $+5\%$ changes in bus voltage. The dc power supply used in experiments had a maximum setting of 400V so the input voltage couldn't be raised to 418V ($380+10\%$).



(a)



(b)

Figure 22: Response of converter to changes in line voltage (a) E reduced to 342V (b) E increased to 400V.

Figure 23 shows the efficiency of the converter over load range and at different bus voltage levels. The maximum efficiency at nominal bus voltage of 380V is 88.02% observed at full load. The efficiency measurements included the losses in input capacitor. The prototype POL converter has lower efficiency compared to commercially available converters. Efficiency can be improved by using a printed circuit board to reduce

parasitic losses. Slight improvements in efficiency can also be realized by using one of the lossless current sensing techniques discussed in [44].

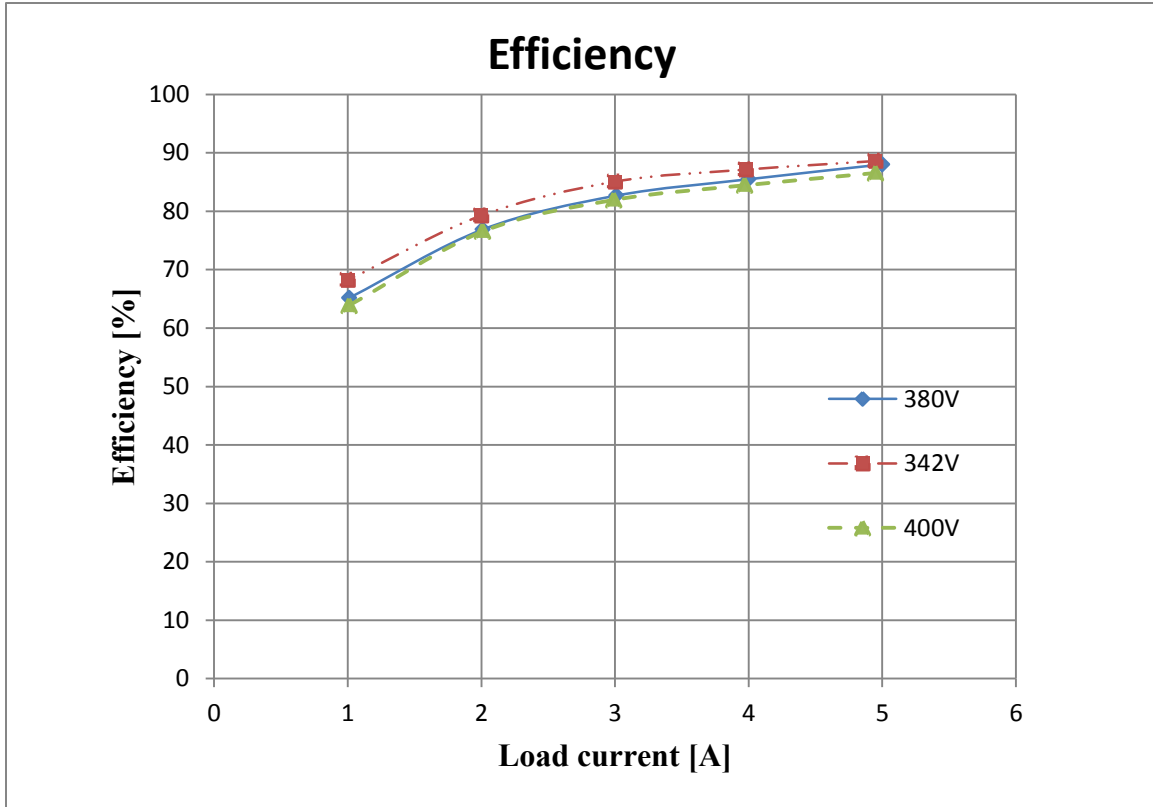


Figure 23: Converter efficiency over load range and at different bus voltage levels.

The converter has an efficiency of 65% at 20% of rated load. As stated in earlier discussions, light load efficiency is an important parameter for POL converters in residential distribution systems. Pulse-skipping and other variable frequency control schemes need to be studied and implemented for POL converters to improve light load efficiency [45].

Chapter 5: System Simulation Results

Using the converter simulation models, a residential dc distribution system is simulated using the SimPowerSystems toolbox in MATLAB. The simulated system is shown in Figure 24. A direct 380V dc connection from utility is assumed so central ac-dc rectifier is not considered in this simulation. The wire is considered to have an inductance of $10\mu\text{H}$ and a resistance of $5\text{m}\Omega$. The input filter for each POL converter consists of $10\mu\text{H}$ inductor with a resistance of $5\text{m}\Omega$ and a capacitor of $1400\mu\text{F}$ with ESR of $5\text{m}\Omega$. Three different POL converters are used in simulation. POL1 is a buck converter for heating loads with 100V output. POL2 is the flyback converter for LED lighting loads with 24V output. POL3 is a 48V buck converter for consumer electronic loads like TV, computers etc. The control for POL3 is same as that for POL1 discussed in section 3.1.2. Non-idealities in the converter components are included in simulations. The heating load is simulated as a constant resistor while the LED model shown in Figure 6 is used at the output of POL2. The electronic load is simulated as a constant resistor with a current source in parallel.

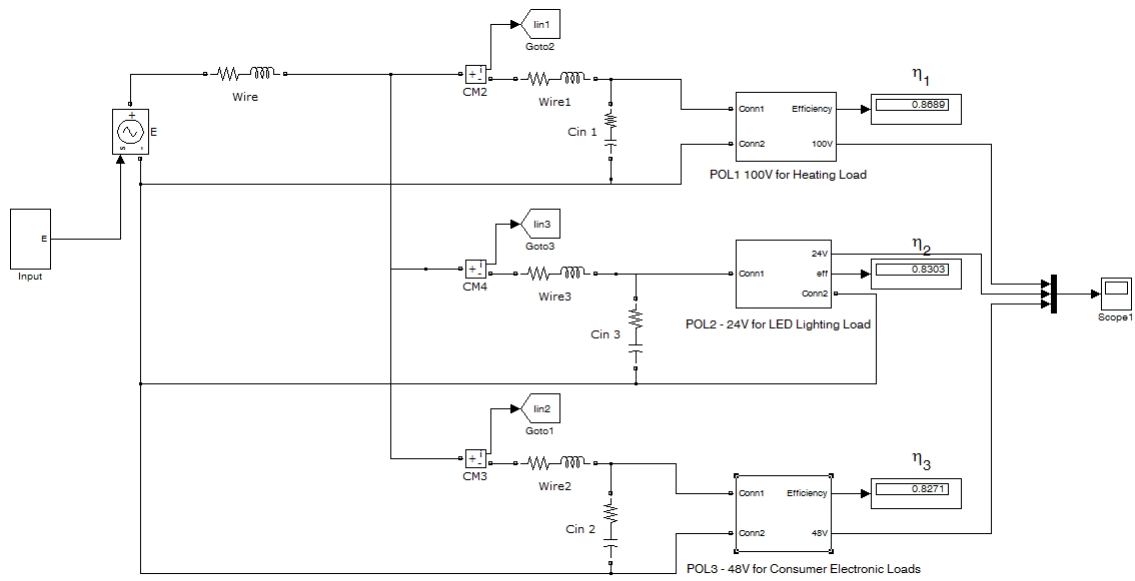


Figure 24: DC distribution system with POL converters.

The response during start-up is shown in Figure 25. A slight overshoot is seen in the outputs of POL1 and POL3 converters. The settling time for the buck converters is 4ms while for the flyback converter is 1ms.

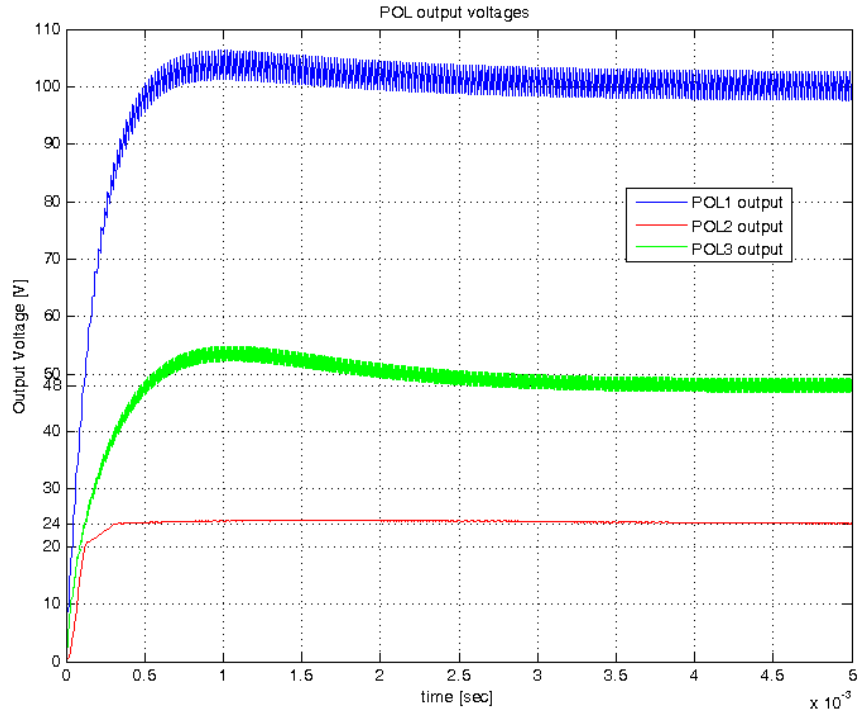


Figure 25: Output voltage of the POL converters.

Figure 26 shows the transient performance of the converters due to a 10% step change in the input voltage. The line regulation of POL converters is important as it allows for the high voltage bus to have wider variation. In this work the 380V dc bus is allowed a deviation of $\pm 10\%$ i.e. 342V – 418V. Figure 27 shows the voltage when electronic load at the output of POL3 converter increases from 5A to 10A at 1A/ μ s. The voltage drops by about 25% and settles to its nominal value in 3msec. The transient performance can be improved by adding additional output capacitors or by using interleaved buck converter.

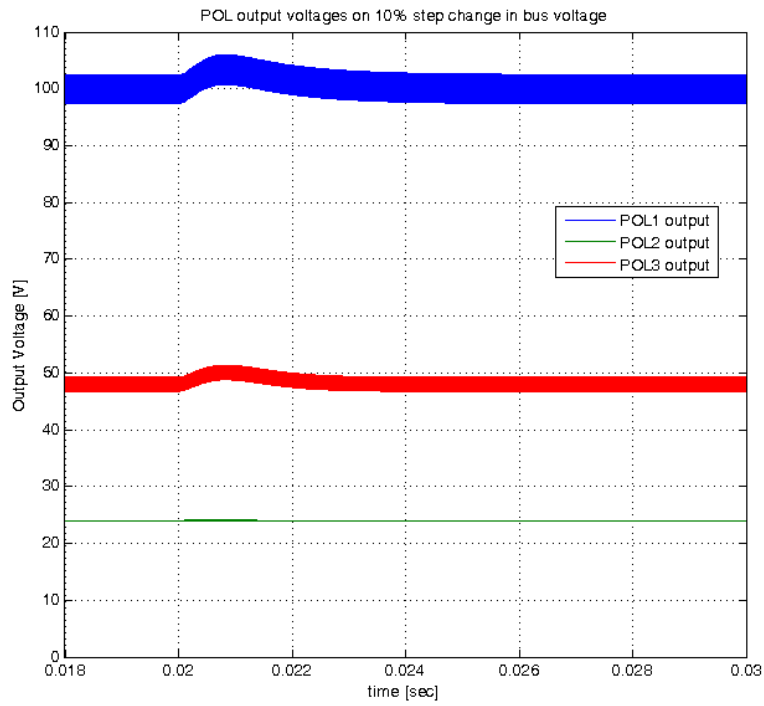


Figure 26: Voltage response after 10% step change in bus voltage.

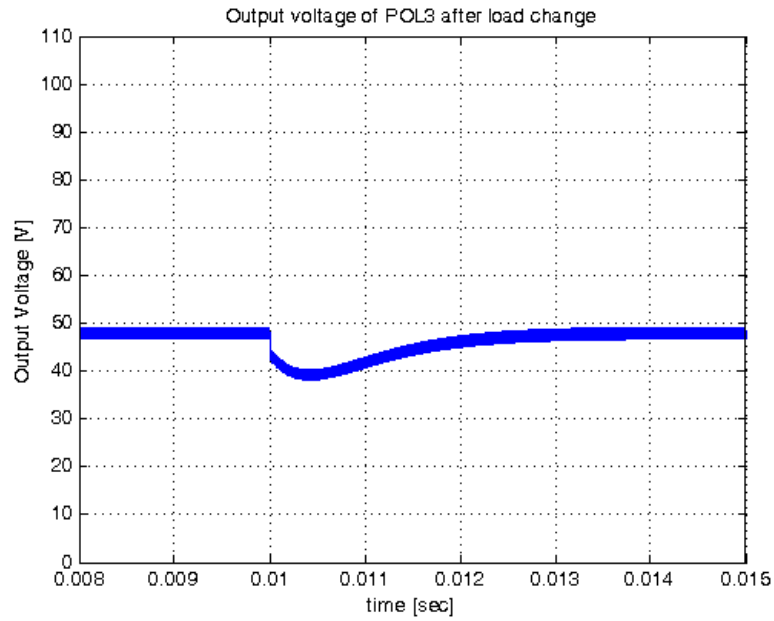


Figure 27: Output of POL3 converter after load increase of 5A at 1A/ μ s.

The steady state efficiencies of the converters are shown in Table 4. The efficiency measurements include the losses in input filter of each converter. The efficiencies are on the lower side and can be improved by using better devices.

Table 4: Efficiencies of individual POL converters at full load.

Converter	Efficiency (%)	Output voltage (V)	Load connected
POL1	86.89	100	Heating load
POL2	83.03	24	LED lighting load
POL3	82.71	48	Electronic load

A residential dc distribution system with 3 POL converters was simulated and the results are as expected. The POL converters have stable response for changes in load and for changes in the bus voltage. The efficiencies at full load are relatively low and can be improved. The efficiency under light loading conditions needs to be improved by using variable frequency control techniques.

Chapter 6: Conclusions

The growth of inherently dc loads, interest in incorporating distributed energy resources (DERs) at consumer premises and advancements in power electronic converters are major reasons to reevaluate the existing residential power distribution system. This thesis has studied residential dc distribution system with primary focus on point-of-load (POL) converters in such a distribution system. The feasibility and effectiveness of dc distribution at small scale such as computer motherboard systems, ships, airplanes, telecom centers and data centers has already been demonstrated. This work suggests expanding it to homes to improve the efficiency of residential power distribution. In a dc distribution system, the dc loads can be connected to the central bus through single stage dc-dc converters thus reducing power loss in intermediate stages like PFC. Future DERs can be easily paralleled to provide local generation and short-term energy storage.

A distributed cascaded architecture is suggested as a suitable candidate for residential dc distribution system. Such architecture allows for improved efficiency and better voltage regulation at the point-of-load. The lack of voltage standard for the central voltage bus and safety concerns are identified as major issues in wide spread adoption of dc distribution systems. A 380V dc bus is considered in this study as it is an intermediate voltage level in most of existing electronic components and allows for cost savings from smaller conductor size. Literature studied suggests the safety from an electric arc in dc system is not an immediate problem however; it is important considering the reliability of electric contacts and connectors.

Common domestic loads are surveyed and characterized. These are classified as heating, inductive and electronic. Heating loads are modeled as a resistor and used in simulation and experiments. Some of the electronic loads act as constant power loads and

introduce instabilities in the system in form of large oscillations or voltage collapse. Stabilizing controllers must be designed for converters supplying electronic loads to avoid instabilities. LED load is modeled as a voltage source with series resistance in simulation studies. A POL buck converter for heating loads with state-feedback and integral control is tested and successfully implemented. The prototype converter has an efficiency of about 88% at rated load which can be further improved. Since majority of the domestic loads operate at low load or are in standby mode, the light load efficiency of POL converters is an important parameter that must be considered in future work.

Using the simulation models of POL converters a small dc distribution system is simulated using MATLAB. Heating, LED lighting and electronic loads are used in the simulation. The results show stable performance of the converters in presence of line and load changes. The efficiencies including losses in input filters are in the range of 82% - 87%.

In future work a system considering various other loads can be designed and implemented. Source converters for DERs and bi-directional converters for energy storage devices can be incorporated along with grid side ac-dc rectifier. The POL converters act as constant power loads for these upstream converters and this makes the study of control of upstream converters important from the perspective of system stability. Appropriate fault detection and mitigation techniques must be included for safe operation. Efficiency of POL converters at light load can be improved using variable frequency and other control techniques. The POL converters can be used for current monitoring and overcurrent protection eliminating the need for passive electromechanical protective devices. Active protection schemes can be realized by using alert mechanisms and other communication protocols between the source and load converters.

References

- [1] D. Nilsson, "DC distribution systems," Licentiate of Engineering Thesis, Division of Electric Power Engineering, Department of Energy and Environment, Chalmers University of Technology, 2005.
- [2] D. Boroyevich, I. Cvetkovic, D. Dong, R. Burgos, F. Wang, F. Lee, "Future electronic power distribution systems a contemplative view," *12th International Conference on Optimization of Electrical and Electronic Equipment (OPTIM)*, pp.1369-1380, May 2010.
- [3] G. Postiglione, "DC distribution system for home and office," Department of Electric Power Engineering, Chalmers University of Technology, October 2001.
- [4] D. Salomonsson, A. Sannino, "Low-voltage DC distribution system for commercial power systems with sensitive electronic loads," *IEEE Transactions on Power Delivery*, vol.22, no.3, pp.1620-1627, July 2007
- [5] G. Seo, J. Baek, K. Choi, H. Bae, B. Cho, "Modeling and analysis of DC distribution systems," *2011 IEEE 8th International Conference on Power Electronics and ECCE Asia (ICPE & ECCE)*, pp.223-227, May -June 2011
- [6] Otero M.; "Power Quality Issues and Feasibility Study in a DC Residential Renewable Energy System," MS Thesis, University of Puerto Rico, 2008.
- [7] A. Kwasinski, "A microgrid architecture with multiple-input dc/dc converters: applications, reliability, system operation, and control," PhD Dissertation, Department of Electrical and Computer Engineering, University of Illinois at Urbana-Champaign, 2007.
- [8] K. Garbesi, V. Vossoss, A. Sanstad, G. Burch, "Optimizing energy savings from direct-DC in US residential buildings," Lawrence Berkeley National Lab, October 2011.
- [9] IEEE Global History Network, "Pearl Street Station" retrieved on 12/12/2011 from <http://www.ieeeahn.org/wiki/index.php/Pearl_Street_Station>
- [10] W. Tabisz, M. Jovanovic, F. Lee, "Present and future of distributed power systems," *Conference Proceedings of Seventh Annual Applied Power Electronics Conference and Exposition (APEC '92) 1992*, pp.11-18, February 1992.
- [11] A. Kwasinski, "Advanced power electronics enabled distribution architectures: Design, operation, and control," *IEEE 8th International Conference on Power Electronics and ECCE Asia (ICPE & ECCE), 2011*, pp.1484-1491, May - June 2011.
- [12] K. Engelen, E. Leung Shun, P. Vermeyen, I. Pardon, R. D'hulst, J. Driesen, R. Belmans, "The Feasibility of Small-Scale Residential DC Distribution

- Systems,” *IECON 2006 - 32nd Annual Conference on IEEE Industrial Electronics*, pp.2618-2623, November 2006.
- [13] D. Nilsson, A. Sannino, “Efficiency analysis of low- and medium- voltage DC distribution systems,” *IEEE Power Engineering Society General Meeting, 2004*, pp.2315-2321 Vol.2, June 2004.
 - [14] “ETSI EN 300 132-3-0 V2.1.1 (2011-10). European Standard (Telecommunications series) Environmental Engineering (EE); Power supply interface at the input to telecommunications equipment; Part 3: Operated by rectified current source alternating current source or direct current source up to 400 V,” European Telecommunications Standards Institute, October 2011.
 - [15] IEC Standardization Management Board Strategic Group 4 (IEC SMB SG4), “LVDC distribution systems up to 1500V DC”, 2009.
 - [16] “Introduction to the IEC SMB SG 4 workshop on LVDC” retrieved on 1/31/2012 from (www.vde.com/en/dke/dkework/newsfromthecommittees/2011/documents/1.pdf)
 - [17] J. Ahn, K. Koo, D. Kim, B. Lee, H. Jin, “Comparative analysis and safety standard guideline of AC and DC supplied home appliances,” *IEEE 8th International Conference on Power Electronics and ECCE Asia (ICPE & ECCE), 2011*, pp.1118-1125, May – June 2011.
 - [18] D. Symanski, “Residential and commercial use of DC power,” EPRI, presented at NEMA, UL & NFPA - Low Voltage Direct Current Workshop, Arlington, VA, April 2011 retrieved online on 12/10/2011 from (www.emergealliance.org/imwp/download.asp?ContentID=20144)
 - [19] EMerge Alliance, “Public Overview of the EMerge alliance standard,” 2008-2009, retrieved online on 1/31/2012 from (<http://www.emergealliance.org/Standard/StandardDownload.aspx>).
 - [20] A. Kwasinski, “Evaluation of dc Voltage Levels for Integrated Information Technology and Telecom Power Architectures,” *4th International Conference on Telecommunication - Energy Special Conference (TELESCON), 2009*, pp.1-7, May 2009.
 - [21] K. Garbesi, V. Vossoss, H. Shen, “Catalog of DC appliances and power systems,” Lawrence Berkeley National Lab, October 2011.
 - [22] Y. Huang, F. Peng, J. Wang, D. Yoo, “Survey of the Power Conditioning System for PV Power Generation,” *37th IEEE Power Electronics Specialists Conference, 2006 (PESC '06)*, pp.1-6, June 2006.
 - [23] SAE International, “Understanding charging speeds: SAE Charging Configurations and Ratings Terminology,” 2011, retrieved online on 1/31/2012 from (<http://www.sae.org/smartgrid/chargingspeeds.pdf>).

- [24] www.chademo.com accessed on 1/31/2012.
- [25] Po-Wa Lee, Yim-Zhu Lee, Bo-Tao Lin, "Power distribution systems for future homes," *Proc. of the IEEE 1999 International Conf. on Power Electronics and Drive Systems, 1999 (PEDS '99)*, vol.2, pp.1140-1146, July 1999
- [26] H. Estes, A. Kwasinski, R. Hebner, F. Uriarte, A. Gattozzi, "Open series fault comparison in AC & DC micro-grid architectures," *IEEE 33rd International Telecommunications Energy Conference (INTELEC), 2011*, pp.1-6, October 2011.
- [27] D. Nilsson, A. Sannino, "Load modelling for steady-state and transient analysis of low-voltage dc systems," *Conf. Rec. of the 39th IAS Annual Meeting, 2004*. vol.2, pp. 774- 780, October 2004.
- [28] J. Baek, S. Gab-Su, C. Kyusik, P. Cheol-Woo, K. Hyejin, B. Hyunsu, H. Bo, "DC Distribution system design and implementation for Green Building," *Green Building Power Forum (GBPF 2011), 2011*, San Jose, CA.
- [29] A. Kwasinski, C. Onwuchekwa, "Dynamic behavior and stabilization of DC microgrids with instantaneous constant-power loads," *IEEE Transactions on Power Electronics*, vol.26, no.3, pp.822-834, March 2011
- [30] Product guide, "All in 1 LED Lighting Solutions Guide," Future Lighting Solutions, July 2011, retrieved online on 12/12/2011 (http://www.futurelightingsolutions.com/en/information-center/literature-library/Documents/led_solutions_guide.pdf)
- [31] S. Ang, and A. Olivia, *Power-Switching converters*, 3rd edition, Boca Raton, CRC Press, 2011.
- [32] E. Mineiro, C. Postiglione, R. Santiago, F. Antunes, A. Perin, "Self-oscillating flyback driver for power LEDs," *Energy Conversion Congress and Exposition, 2009 (IEEE ECCE 2009)*, pp.2827-2832, September 2009.
- [33] A. Kwasinski, Course materials for EE 394V Distributed Generation Technologies, Fall 2010.
- [34] A. Kwasinski, Course materials for EE 394V Advanced Power Electronics, Fall 2009.
- [35] A. Oliva, S. Ang, G. Bortolotto, "Digital control of a voltage-mode synchronous buck converter," *IEEE Transactions on Power Electronics*, vol.21, no.1, pp. 157-163, January 2006.
- [36] R. Vaccaro, *Digital Control: A State-Space Approach*, New York, McGraw-Hill, 1995.
- [37] J. Van de Vegte, *Feedback Control Systems*, Englewood Cliffs, Prentice-Hall, Inc., 1986.

- [38] G. Sauerlander, D. Hente, H. Radermacher, E. Waffenschmidt, J. Jacobs, "Driver Electronics for LEDs," *Conf. Rec. of the 41st IAS Annual Meeting, 2006*, vol.5, pp.2621-2626, October 2006.
- [39] H. van der Broeck, G. Sauerlander, M. Wendt, "Power driver topologies and control schemes for LEDs," *Twenty Second Annual IEEE Applied Power Electronics Conference, APEC 2007*, pp.1319-1325, February 2007-March 2007.
- [40] R. Erickson and D. Maksimovic, *Fundamentals of Power Electronics*, 2nd ed. New York, Springer, 2001.
- [41] L. Dixon, "Average Current Mode Control of Switching Power Supplies," Unitrode Application Note, retrieved online on 1/12/2011 (<http://www.ti.com/lit/an/slua079/slua079.pdf>)
- [42] T. Chern, L. Liu, C. Huang, Y. Chern, J Kuang, "High power factor Flyback converter for LED driver with Boundary Conduction Mode control," *5th IEEE Conf. on Industrial Electronics and Applications (ICIEA), 2010*, pp.2088-2093, June 2010.
- [43] Pang, H.M., Bryan, P.M.H., "A stability issue with current mode control flyback converter driving LEDs," *6th International Power Electronics and Motion Control Conference, 2009 (IPEMC '09)*, pp.1402-1406, May 2009.
- [44] H. Forghani-zadeh, G. Rincon-Mora, "Current-sensing techniques for DC-DC converters," *The 45th Midwest Symposium on Circuits and Systems, 2002. MWSCAS-2002.*, vol.2, pp. II-577- II-580, August 2002.
- [45] A. Chakraborty, A. Pfaelzer, "An overview of standby power management in electrical and electronic power devices and appliances to improve the overall energy efficiency in creating a green world," *Journal of Renewable and Sustainable Energy*, Vol. 3, Issue 2, April 2011.

Vita

Harshad Desai was born in Sangli, Maharashtra, India. Upon completion of his schooling in Pune, he pursued Bachelor's degree in Electrical and Electronics Engineering from National Institute of Technology Calicut, Kerala, India. He started his graduate studies at the University of Texas at Austin in fall 2009. He is currently interested in power electronics and control systems.

Email: harshaddesai@utexas.edu

This thesis was typed by Harshad Desai.